Journal of Hydrology 566 (2018) 1–22

Contents lists available at ScienceDirect

Journal of Hydrology

journal homepage: www.elsevier.com/locate/jhydrol

Research papers

Hydrologic impacts of climate change: Comparisons between hydrological parameter uncertainty and climate model uncertainty

Jisha Joseph[a], Subimal Ghosh[a,b,*], Amey Pathak[a], A.K. Sahai[c]

[a] Department of Civil Engineering, Indian Institute of Technology Bombay, Mumbai 400 076, India
[b] Interdisciplinary Program in Climate Studies, Indian Institute of Technology Bombay, Mumbai 400 076, India
[c] Indian Institute of Tropical Meteorology, Dr. Homi Bhabha Road, Pashan, Panchawati, Pune, Maharashtra 411008, India

ARTICLE INFO

This manuscript was handled by C. Corradini, Editor-in-Chief, with the assistance of Corrado Corradini, Associate Editor

Keywords:
Climate change
Hydrologic impacts
Uncertainty
Parameter uncertainty
Hydrologic model of large basin

ABSTRACT

Assessing impacts of climate change on hydrology involves global scale climate projections by General Circulation Models (GCMs), downscaling of global scale projections to regional scale by statistical methods or regional climate models and then use of regional outputs in hydrological simulations. Hydrological simulations considers varying inputs starting with soil characteristics, land cover, vegetation types, control structures to social parameters such as human interventions, irrigation and water use. This makes the model highly parametrized and at the same time highly uncertain due to the non-availability of majority of input parameters. Here, we compare the contributions of uncertainty from hydrological parameterization in the hydrological projections of climate change to that generated from the use of multiple climate models. The Ganga River Basin in India was selected as the study region. For regional climate change projections, we use dynamic downscaling outputs from Coordinated Regional Climate Downscaling Experiment (CORDEX) and statistical downscaling outputs from a transfer function forced with 3 GCMs, Institut Pierre Simon Laplace (IPSL), European Consortium Earth System Model (EC-EARTH) and MPI (Max Plank Institut) ESM (Earth System Model). Monte-Carlo Simulations (MCS) are performed with 1000 generated sets of sensitive model parameters for each of the GCM-regional model combination. We find that the observed time series of river discharge is reproduced well but with bias in low-flow conditions. This is probably associated with human intervention and poor representation of baseflow in VIC due to the neglected groundwater storage which feed the surface water during low flow condition. The future projections show that the major uncertainty lies across climate models for all the four seasons (MAM, JJAS, ON and DJF) and for all the hydrological variables, soil moisture, evapotranspiration (ET), water yield and river discharge. The uncertainty resulting from the MCS is quite small as compared to the climate model uncertainty. We are unable to find any added value in hydrological simulations by rigorous hydrological calibration and parameterization in absence of many required data, when the forcing meteorological data has huge uncertainty. Our findings highlight the need of convergence of climate models before the studies on hydrological impacts assessment and subsequent development of adaptation strategies.

1. Introduction

The study of regional hydrologic implications of changing climate has crucial role in the management of water resources. The water cycle is expected to be accelerated as a result of the increase in temperature (Oki and Kanae, 2006). The intensity, frequency and duration of precipitation events are expected to change with warming (Kumar et al., 1992; Trenberth et al., 2003; Wild and Liepert, 2010). Evapotranspiration, soil moisture and runoff are highly sensitive to even small changes in temperature and precipitation (Chattopadhyay and Hulme, 1997; Milly et al., 2005; Seneviratne et al., 2010). GCMs provide the information about the future climate by simulating time series of climate variables with greenhouse gas effect over the atmosphere (Prudhomme et al., 2003). However, GCMs are at very coarse resolution and for regional climate change impact studies, it has to be brought to finer scale by downscaling. Regional hydroclimatic modelling hence involves the following steps: simulating the future climate variables using GCMs, downscaling the outputs to basin scale and using this as forcing to hydrological models for assessing hydrological impacts of climate change. A number of hydrological models based on water and energy balances, have been developed in the recent past for this purpose (Arnell, 1999; Döll et al., 2003; Gleick, 1986; Liang et al., 1996,

* Corresponding author at: Department of Civil Engineering, Indian Institute of Technology Bombay, Mumbai 400076, India.
E-mail address: subimal@civil.iitb.ac.in (S. Ghosh).

https://doi.org/10.1016/j.jhydrol.2018.08.080
Received 26 July 2018; Received in revised form 26 August 2018; Accepted 30 August 2018
Available online 04 September 2018

Table 1
Previous uncertainty assessment studies.

Reference	Details of uncertainty assessment
Bastola et al. (2011)	Sources of uncertainty considered: GCMs, emission scenario, model parametrisation, model structure Hydrological variables considered: streamflow Calibration performed: Yes Out of 5 sensitive parameters only 2 were considered to be uncertain • different techniques of uncertainty assessment (viz. Generalised Likelihood uncertainty assessment and Bayesian Model Averaging) were used
Bergström et al. (2001)	Sources of uncertainty considered: GCMs, RCMs, two versions of the same model Hydrological variables considered: river discharge, ET Calibration performed: Yes • Calibration is performed for both the model employed for the study hence not considering the model parameter uncertainty
Chen et al. (2011a,b)	Sources of uncertainty considered: GCMs, statistical downscaling technique, model structure Hydrological variables considered: river discharge Calibration performed: Yes • Calibration is performed for both the model employed for the study hence not considering the model parameter uncertainty
Crosbie et al. (2011)	Sources of uncertainty considered: GCMs, choice of downscaling and model structure Hydrological variables considered: recharge Calibration performed: Yes • The groundwater recharge is given the main emphasis for uncertainty assessment and model parameter uncertainty is not taken into account
Dobler et al. (2012)	Sources of uncertainty considered: GCMs, RCMs, bias correction, model parameters Hydrological variables considered: river discharge Calibration performed: Yes • 20 parameter sets with highest NSE are selected for the assessment
Jiang et al. (2007)	Sources of uncertainty considered: model structure Hydrological variables considered: streamflow, ET and soil moisture Calibration performed: Yes • 6 monthly water balance model and 15 hypothesized climate change scenarios were considered
Moeck et al. (2016)	Sources of uncertainty considered: GCMs, RCMs, model parametrisation, model structure, observed data for calibration Hydrological variables considered: recharge Calibration performed: Yes • Considering one model as the reference, other models were calibrated with respect to its outputs
Prudhomme et al. (2003), Maurer and Duffy (2005)	Sources of uncertainty considered: GCMs Hydrological variables considered: streamflow Calibration performed: Yes
Raje and Krishnan (2012)	Sources of uncertainty considered: GCMs, model parametrisation Hydrological variables considered: streamflow, ET and soil moisture Calibration performed: Yes • GCMs are interpolated and bias corrected instead of downscaling
Stoll et al. (2011)	Sources of uncertainty considered: GCMs, RCMs, bias correction techniques Hydrological variables considered: annual recharge, ET and hydraulic head Calibration performed: Yes • Bias correction is performed for both precipitation and potential ET • The uncertainty assessment is carried out for calibrated model parameters hence neglecting the model parameter uncertainty
Teng et al. (2012)	Sources of uncertainty considered: GCMs, model structure Hydrological variables considered: streamflow Calibration performed: Yes
Teutschbein et al. (2011)	Sources of uncertainty considered: GCMs, statistical downscaling techniques, emission scenario, model parameters Hydrological variables considered: river discharge, flood peak Calibration performed: Yes • 100 optimised set of parameters generated during calibration was used for the uncertainty assessment
Wilby and Harris (2006)	Sources of uncertainty considered: GCMs, statistical downscaling, model structure Hydrological variables considered: streamflow Calibration performed: Yes • Out of 5 sensitive parameters only 2 were considered to be uncertain
In the present study: Sources of uncertainty considered: GCMs, downscaling method, model parameters Hydrological variables considered: river discharge, ET, soil moisture, water yield Calibration performed: No • All the possible ranges of parameters are taken into account and no calibration is done. • This allows maximum possible uncertainty unlike in other studies that use calibrated parameter sets. The inaccuracies due to erroneous and human intervened observed data are also eliminated	

1994; Vorosmarty and Moore, 1991). Numerous attempts have been made to understand the land surface hydrologic responses to climate change using the macroscale hydrological models for specific geographic locations (Christensen et al., 2004; Hamlet and Lettenmaier, 1999; Lettenmaier and Gan, 1990) including Indian river basins (Singh and Kumar, 1997; Gosain et al., 2006; Raje et al., 2014). The impact assessment however is associated with uncertainties that are involved in each step of hydroclimatic modeling, i.e., uncertainty in GCM projections, downscaling uncertainty and hydrological parameter uncertainty (Leavesley, 1994; Xu, 1999). Representing these uncertainties in climate change impact studies is equally important and at the same time considering all its sources concurrently is challenging.

Multiple number of GCMs have been developed with different algorithms for land-atmosphere-ocean interactions hence giving different

outputs. Therefore, the projected hydrological variables are highly dependent on the GCMs employed in the study. These uncertainties are assessed with the use of information from multiple GCMs (e.g. (Allen et al., 2000; Lee and Kim, 2013; New and Hulme, 2000; Simonovic et al., 2003; Simonovic and Li, 2004; Tebaldi et al., 2005) Some of the approaches to address the uncertainty across climate models include, non-parametric approach (Ghosh and Mujumdar, 2007), possibilistic approach (Mujumdar and Ghosh, 2008), imprecise probability (Ghosh and Mujumdar, 2009), analysis of variance (Hingray et al., 2014; Yip et al., 2011), square root error variance (Woldemeskel et al., 2016, 2014) etc. The above studies provide an interpretation of uncertainties limiting to that arising due to GCMs and not focusing on the other aspects of it. Downscaling techniques can be broadly classified to statistical and dynamical downscaling. In statistical downscaling a data-driven relationship is derived between the predictors (GCM simulated climate variable) and predictands (regional scale variable) (e.g. Conway and Jones, 1998; Chen et al., 2010; Groppelli et al., 2011; Jeong et al., 2012; Osca et al., 2013; Kannan and Ghosh, 2013; Salvi et al., 2013; Sachindra et al., 2013; Santos et al., 2016). Dynamic downscaling makes use of Regional Climate Models (RCMs) (e.g., Jones et al., 1995; Dobler and Ahrens, 2010, 2011; Krishna Kumar et al., 2011; Liu et al., 2013; Dosio et al., 2015; Scinocca et al., 2016). Though both the methods have their own advantages (and limitations), the assumptions involved in it adds to the uncertainty (Fowler et al., 2007). The uncertainty arising due to the use of different methods of statistical downscaling have been modelled in the recent past (Ghosh and Katkar, 2012; Gutmann et al., 2014; Hu et al., 2013; Khan et al., 2006; Samadi et al., 2013). The uncertainty resulting from the use of different observed data used for model calibration in statistical downscaling was studied by Kannan et al. (2014). The assessment of different dynamical downscaling methods (Im et al., 2010; Kumar et al., 2013; Mishra, 2015; Singh et al., 2016) and inter-comparison of statistical and dynamical downscaling techniques (Chen et al., 2011a; Flaounas et al., 2013; Vaittinada Ayar et al., 2016) were also performed in various studies. It can be inferred from the above studies that a major portion of uncertainty is explained by the choice of downscaling method along with the selection of GCMs.

Hydrological models, on the other hand, are highly parametrized, some of which are heterogeneous in space and time or cannot be measured. A number of calibration techniques have been developed which uses observed data as a reference to obtain the approximate value of these parameters (Moradkhani and Sorooshian, 2009; Troy et al., 2008; Yapo et al., 1996). Difficulty in obtaining unique set of parameters, lack of accurate observed data etc. lead to parameter uncertainty in hydrological models. Uncertainty assessment in hydroclimatic simulations involving hydrological models have become recent research trend. Wilby and Harris (2006) proposed a probabilistic framework considering ensemble of 4 GCMs, 2 scenarios, 2 downscaling techniques, 2 hydrological model structures and 2 sets of hydrological model parameters for assessing the uncertainty in climate change impacts on low flow scenario of River Thames, UK. Use of multiple hydrological models is also observed in multiple studies to assess the uncertainty (Teng et al., 2012; Velázquez et al., 2013). Various techniques like multi-objective calibration approach (Ruelland et al., 2015), Generalized Likelihood Uncertainty Estimation (Beven and Binley, 1992), Bayesian Model Averaging (Bastola et al., 2011) technique were utilized for uncertainty assessment. Raje and Krishnan (2012) used the Bayesian approach implemented by Markov Chain Monte Carlo method to assess the uncertainty in VIC model under hydroclimatic studies for Indian River basins. Extensive amount of research has been carried out for the uncertainty assessment of hydrological impacts of climate change by the consideration of multiple GCMs, downscaling techniques, hydrological models and parameters (e.g., Jiang et al., 2007; Bastola et al., 2011; Chen et al., 2011b; Bae et al., 2011; Chen et al., 2012; Bosshard et al., 2013). Apart from the uncertainty assessment, few studies aim at evaluating the extent to which the climate change adaptation strategies are affected by uncertainty (Refsgaard et al., 2013) and possible ways of reducing it (Raje and Mujumdar, 2009; Refsgaard et al., 2016). Previous uncertainty assessment studies have been summarized in Table 1. As observed in the table, previous studies largely performed hydrologic model calibration based on observed streamflow data and used the same to understand hydrologic model parameter uncertainty. They have used either statistical or dynamic downscaling or a simple bias correction without downscaling, though there have been a consistent finding that GCM uncertainty dominates.

Global and regional hydrological cycle has been significantly affected by human interventions (Jaramillo and Destouni, 2015) such as, irrigation, reservoir operation, ground water pumping and majority of the available Land Surface Models (LSMs) are unable to simulate all of them together (Haddeland et al., 2006a, 2006b; Leng et al., 2014; Rosenberg et al., 2013). Furthermore there is often non-availability of data pertaining to the same. Hence, the hydrologic model calibration for Indian case studies is extremely difficult and often erroneous because, models can not consider the water regulation due to non-availability of data. Models, without accounting for water regulation, consider observed flows for calibration, but these flows are regulated flows in India. Hence, such a calibration may capture the streamflow, but for a wrong reason (e.g., Döll et al., 2008; Raje et al., 2014; Syed et al., 2014;Chawla and Mujumdar, 2015). The other set of studies use the recommended values of parameters without a specific calibration (Mishra et al., 2010) and they have been criticized to misrepresent the hydrological system with uncalibrated parameters; though not tested through a proper framework. Rather than going for an erroneous model calibration due to lack of available data, the hydrologic model parameters were allowed to consider any possible value. This allows maximum possible uncertainty due to parameterization which is of much higher magnitude than any other estimation of uncertainty incorporating calibration. Even such an uncertainty remains insignificant with respect to the climate model uncertainty and this raises a very important question on the readiness of using such uncertain projections for climate change adaptation. This specific science question has not been addressed in any of the available literature for large river basins in South Asia. Further to this, the analysis was not limited just with streamflow (as the majority of available streamflow data are regulated), but considered other variables, such as soil moisture and ET to understand the complete picture of changing water cycle. Unlike other studies, we have not considered only a single suit of downscaling, rather considered both statistical and dynamic downscaling to present the complete picture of uncertainty.

This analysis is an advancement with respect to other studies in terms of

i. consideration of complete uncertainty from multiple GCMs and downscaling methods;
ii. assessing multiple hydrologic variables to understand changing pattern of the water cycle
iii. allowing maximum possible uncertainty in hydrologic parameterization to show the significance of climate model uncertainty and finally
iv. checking the adequacy and preparedness of climate models to be used in hydrologic impacts assessment.

Here we address the science question on the impacts of hydrological parameter uncertainty in the background of GCM and downscaling uncertainty. We attempt to compare and understand the contribution of uncertainty from climate models and hydrologic parameterization to the hydroclimatic projections with a case study application of Ganga River basin, India. The Variable Infiltration Capacity (VIC) model which is a semi-distributed macroscale hydrological model is implemented for this purpose. The major objectives of the study are:

i. to assess the uncertainty in hydrologic impacts of climate change

over Ganga basin, in the context of GCM uncertainty, downscaling uncertainty and parameter uncertainty

ii. to render the spread of climate induced changes in output variables (streamflow, ET, soil moisture and water yield) from all the possible values of the uncertain parameters in VIC model and compare it with GCM and downscaling uncertainty

We use MCS with the VIC model considering the sensitive parameters to be uncertain. Selection of sensitive parameters is performed based on earlier studies (Demaria et al., 2007). We assume that soil parameters follow triangular distribution (Muleta and Nicklow, 2005) where the mode is the recommended value of the parameters and the base of the triangles are the possible ranges. The vegetation parameters are considered to follow uniform distribution within a range of ± 0.1 times the prescribed value, since the ranges were unknown. Random numbers are generated for each of the parameters using these distributions and ranges. The dynamic downscaled (CORDEX) and statistical downscaled (transfer function) outputs of 3 GCMs, IPSL, EC-EARTH and MPI ESM are used as meteorological forcings. For each of the GCM-downscaling combination, MCS are performed for the VIC model using 1000 generated sets of parameters. The results are compared for the assessment of uncertainty. The following section presents the details of data and methodology used.

2. Data and methodology

2.1. Study area

The Ganga Basin located within the geographical coordinates of 73°30′E to 89°0′E latitude and 22°30′N to 31°30′N longitude, extends over India, Nepal and Bangladesh and covers an area of 1086000 km^2. In India it extends over an area of 861404 km^2 (Fig. 1a.) and receives an annual average rainfall of 110 cm. The monsoon months are from June to September with rainfall spatially varying from 39 to 200 cm (NRCD MoEF, 2009). The Ganga River is snow-fed and hence maintains a moderate level of streamflow throughout the year with maximum discharge during the monsoon months causing flood in the plains. The Ganga Basin is characterised by large variation in altitude ranging from 7000 m at the Himalayan Mountains to 50 m in the Gangetic Plain. It is the largest and most cultivated basin in the country with dense population. The land use land cover over the region is shown in Fig. 1(b). There is an increase in the water demand for the last few decades to meet the needs of growing population posing a stress to surface water and groundwater hence making the climate change studies inevitable for this basin.

2.2. Regional climate model simulations

The dynamically and statistically downscaled output of 3 GCMs, IPSL, EC-EARTH and MPI ESM are considered for climate change projections. The CORDEX simulations are used as dynamic downscaling output, where RCMs were forced with lateral boundaries from global IPSL, EC-EARTH and MPI ESM and run at a resolution of 50 km over the CORDEX South Asian domain. The regional models used for downscaling are Regional Climatic Model version 4 (RegCM4) for IPSL, Rossby Centre regional atmospheric model version 4 (RCA4) for EC-EARTH (Singh et al., 2016) and REMO (Regional Model) 2009 for MPI ESM. The output of these runs were acquired from the CORDEX South Asia group (http://cccr.tropmet.res.in/home/index.jsp) at daily scale. The Representative Concentration Pathway (RCP 4.5) emission scenario, which is a midrange scenario (Taylor et al., 2012), is considered. The choice of the GCM was based on the availability of their output. Among the CORDEX regional simulations for South Asia, provided by Centre for Climate Change Research (CCCR), only IPSL, EC-EARTH and MPI have surface wind speed data for historical as well as future (RCP 45) time period. We use both the simulations for historical period (1979–2005) and future period (2011–2037). The RCM simulated climate variables may have realistic spatial patterns but have bias from the observed value and need to be corrected. Here, we perform the same by quantile based bias correction method developed by Li et al. (2010). The observed data used as reference is Indian Meteorological Department (IMD) gridded data products of precipitation (Rajeevan et al., 2006; Rajeevan and Bhate, 2009) and temperature (Srivastava et al., 2009). IMD had rainfall observations at 6076 stations for varying time intervals. The dataset was developed using about 3500 rain gauge stations on an average for daily analysis.

Statistical downscaling method includes the development of an empirical relationship between the predictors (GCM simulated climate variable) and the predictands (regional scale variable). It can be broadly classified into three: weather generators, weather typing and

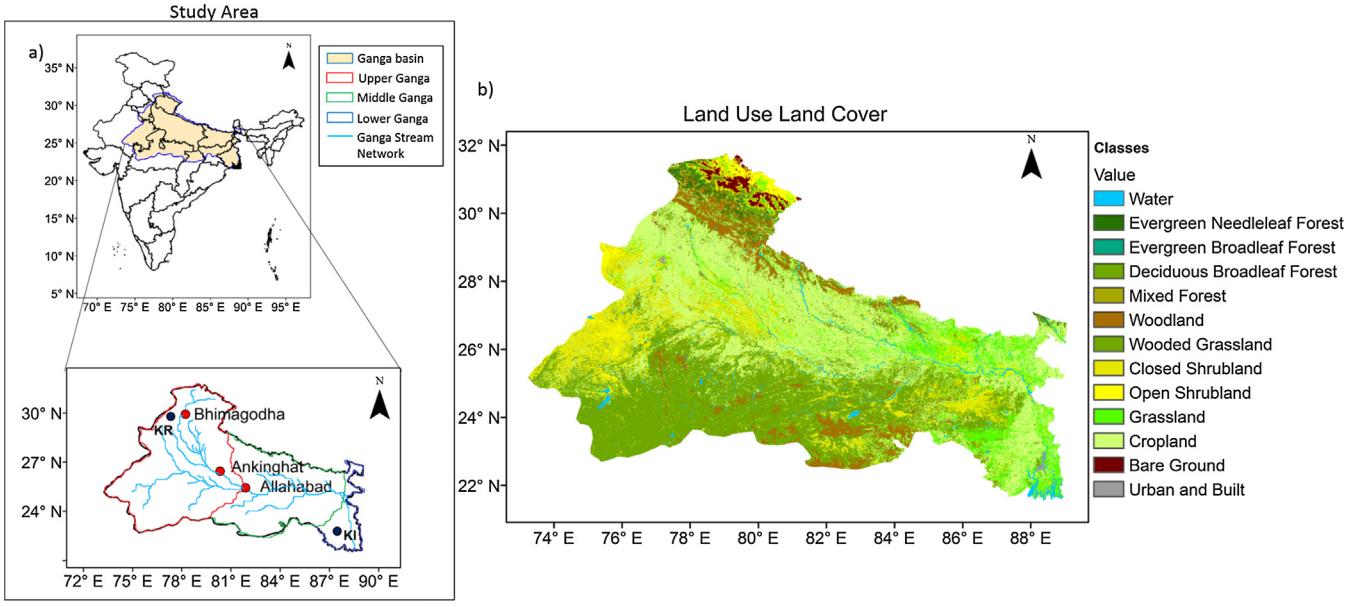

Fig. 1. Location and details of Ganga Basin (a) A map showing the geographical location of Ganga Basin. The streamflow validation points are Ankinghat and Bhimagodha. The soil moisture validation points are KRN (KR) and KLNI (KI). Land use land cover map of Ganga basin (UMD Land Cover Classification) (b) are shown.

Table 2
Parameters in VIC model. In the table, the parameters in bold are the sensitive parameters. We have also performed additional simulations considering all above parameters following uniform distribution and presented the results in supplementary figures. (Figs. S1–S5).

Variable Name (soil parameters)	Description	Range
Soil parameters		
infilt	**Variable infiltration curve parameter (b_i)**	**0.00001–0.5**
Ds	**Fraction of Dsmax where non-linear baseflow begins**	**0.0005–0.5**
Dsmax	**Maximum velocity of baseflow**	**1–30**
Ws	**Fraction of maximum soil moisture where non-linear baseflow occurs**	**0.5–1**
c	Exponent used in baseflow curve	Set to 2
expt	Parameter describing the variation of Ksat with soil moisture	1–3
Ksat	Saturated hydrualic conductivity	163–4765
phi_s	Soil moisture diffusion parameter	–
init_moist	Initial layer moisture content	–
Elev	Average elevation of grid cell	–
depth	**Thickness of each soil moisture layer**	**0.1–1.5**
avg_T	Average soil temperature	–
dp	Soil thermal damping depth	–
bubble	Bubbling pressure of soil	4–45
quartz	Quartz content of soil	–
bulk_density	Bulk density of soil layer	1200–1609
soil_density	Soil particle density	2000–2900
off_gmt	Time zone offset from GMT	–
Wcr_FRACT	Fractional soil moisture content at the critical point (~70% of field capacity)	–
Wpwp_FRACT	Fractional soil moisture content at the wilting point	–
rough	Surface roughness of bare soil	–
snow_rough	Surface roughness of snowpack	–
annual_prec	Average annual precipitation.	–
resid_moist	Soil moisture layer residual moisture.	–
Vegetation Parameters		
root_depth	**Root zone thickness**	**0.1–5**
Root_fract	Fraction of root in the current root zone.	0–1
Vegetation Library		
rarc	Architectural resistance of vegetation type	–
rmin	Minimum stomatal resistance of vegetation type	–
LAI	Leaf-area index of vegetation type	–
albedo	Shortwave albedo for vegetation type	–
rough	Vegetation roughness length	–
displacement	Vegetation displacement height	–
wind_h	Height at which wind speed is measured.	–
RGL	Minimum incoming shortwave radiation at which there will be transpiration.	–
rad_atten	Radiation attenuation factor	–
wind_atten	Wind speed attenuation through the overstory	–
trunk_ratio	Ratio of total tree height that is trunk (no branches)	–

transfer functions. The weather-type models are observed to fail in terms of simulating the spatial variability of the daily precipitation (Conway and Jones, 1998). Although the weather generator models, such as conditional random field by Raje and Mujumdar (2009), overcome the above drawback of weather typing method; they still fail to simulate the mean condition and spatial cross correlations across stations in a given region. It also demands large number of parameters and computational expense. The downscaling model used in the present study involves the use of Kernel Regression coupled with Classification and Regression Tree (CART) developed by Kannan and Ghosh (2013) and Salvi et al. (2013). The main strengths of this method over other available downscaling technique are its ability to capture the cross correlation between the stations and to project the mean rainfall with high accuracy. Salvi et al. (2013) have shown that the orography is also captured well by the model hence performing better in simulating the monsoon in comparison to other downscaling models. As the first step, the variables that directly affect the rainfall processes are selected as the predictors. Temperature, pressure, specific humidity, u-wind and v-wind at surface and 500 HPa pressure level are used as predictors, in the present case. The bias in these predictor variables are corrected with respect to the reanalysis data by National Centers for Environmental Prediction/National Center for Atmospheric Research (NCEP/NCAR) using quantile based mapping technique (Li et al., 2010). The bias corrected data is characterised by multidimensionality and multicollinearity which has to be reduced before using it for statistical downscaling. In order to reduce the number of dimensions with minimum decrease in the variability of data, Principal Component Analysis (PCA) is applied to the bias corrected predictor variables to obtain the principal components. The next step is to classify the days based on the spatial pattern of rainfall in the zone of interest, and we use K-means clustering, as adopted by Kannan and Ghosh (2013). The relationship between the principal components and the rainfall states for the observed period is derived using Classification and Regression Tree (CART), which is a decision tree learning technique. Using the developed relationship and the future principal components from bias corrected GCM simulations, we obtain the rainfall state for the future time period. In order to project the future rainfall from future states, the Kernel regression technique is utilized. The Kernel Regression is a non-parametric technique and can be used to estimate the conditional probability of a random variable. The developed kernel regression in applied to the predictors and derived stated from bias corrected GCM simulations to obtain the daily rainfall projections. For temperature we use direct bias correction techniques and they are more reliable and smoother as compared to rainfall (Hughes et al., 1993).

2.3. Hydrological simulations with variable infiltration capacity model

VIC model is a semi-distributed macroscale hydrological model in which the water and energy balance equations are solved grid wise (Liang et al., 1994). The sub-grid heterogeneity in vegetation is considered by dividing each grid into smaller tiles based on the land cover. VIC also considers variation in the soil moisture capacity at subgrid level, non-linear recession of baseflow and topography that accounts to orographic precipitation and temperature lapse rate. Multiple layers of soil can be considered in VIC but generally it is taken as 3 with first 2 layers showing dynamic response to the infiltrated rainfall and the third layer showing seasonal variation of soil moisture. The runoff occurs from the bottom layer according to ARNO model (please refer Liang et al., 1994 for furtur details). The upward movement of moisture is transported by evapotranspiration through the roots of the vegetation. The evapotranspiration is calculated using Penman-Monteith equation considering it as a function of vapour pressure deficit and net radiation. The interception of rainfall by the canopy is calculated as a function of LAI. The soil properties are considered to be same throughout each grid cell. The model can be run in either water balance or energy balance at daily or sub-daily time step. Once the energy balance and water balance are computed, routing model (Lohmann et al., 1998) is employed to calculate the streamflow using the runoff and baseflow from each grid. Snow module can be kept active to account for snowmelt. Energy balance approach is used to represent the snow accumulation and ablation according to Andreadis et al. (2009). Based on the total capacity of snow, the water holding capacity is defined and the newly intercepted water is calculated with respect to it. The excess of water holding capacity will be the snowmelt. The inputs for VIC model includes meteorological data (precipitation, maximum temperature, minimum temperature and wind), soil properties, land use, vegetation properties and topographical details. The parameters in the model are listed in

Table 2. VIC has been extensively used for climate change and land use change impact studies, drought assessment, hydrological forecasting etc. (Chawla and Mujumdar, 2015; Haddeland et al., 2006b; Mishra et al., 2010; Nijssen et al., 2001a,b; Nijssen et al., 1997).

The VIC model includes certain parameters which cannot be measured in-situ since they are extremely heterogeneous in nature or they are not physically observable. These parameters are usually calibrated by minimising the difference between simulated and observed data. Few of the calibration parameters are:

(i) Dsmax (mm/day): it is the maximum velocity of the baseflow for the lowest layer of soil and it can vary between 0 and 30 depending on hydraulic conductivity. It is calculated by multiplying the slope of the grid cell with saturated hydraulic conductivity.
(ii) Ds (fraction): it is the fraction of Dsmax where non-linear baseflow occurs. It varies in the range of 0–1 and an initial value of 0.001 can be assumed. With high Ds in the bottom soil layer and with lower water content, the baseflow is high. The baseflow parameter is highly sensitive in basins with snow accumulation and snowmelt (Raje and Krishnan, 2012).
(iii) Ws (fraction): it is the maximum soil moisture at the lowest layer where non-linear baseflow occurs and is analogous to Ds. The runoff peaks get delayed with higher value of Ws, since the water content will be raised with rapidly increasing the non-linear baseflow. Its value is in the range of 0–1, generally greater than 0.5.
(iv) binf: it denotes the shape of the Variable Infiltration Capacity curve. The available infiltration capacity is linked to the relative saturated grid cell area by this parameter. It varies between 0 and 0.4. High value of binf leads to high infiltration and low surface runoff. The partitioning of rainfall (snowmelt) to direct runoff and infiltration is hence controlled by this parameter.
(v) Soil depth (m) -the soil depth of second and the third layers are considered for calibration and they are in the range of 0.1–1.5 m. As the soil depth increases, the seasonal peak flows get delayed and the evapotranspiration increases.

In the present study, apart from the soil parameters, few of the vegetation parameters were also considered to be sensitive. Leaf Area Index (LAI), rooting depth, vegetation roughness length and vegetation displacement height are regarded to be uncertain following a uniform distribution.

2.3.1. Data used in VIC

The topographic details are derived from Digital Elevation Map (DEM) from U.S. Geological Survey (USGS) HYDRO1k dataset at 1 km resolution (https://lta.cr.usgs.gov/HYDRO1K, Raje et al., 2014). The Land Use Land Cover (LULC) data are acquired from the Advanced Very High Resolution Radiometer(AVHRR) available at the website of University of Maryland at a spatial resolution of 1 km (Hansen et al., 2000; Raje et al., 2014). The values of soil parameters were directly procured from the 0.5° global input parameter, available at the VIC model website. The soil file is the interpolated version of the 2° degree global file developed by Nijssen et al. (2001a,b) which was prepared using soil map by Food and Agricultural Organisation (1995). The sub sampling was carried using nearest neighbourhood approach. The metrological data required for running the VIC model are rainfall, air temperature extremes and wind speed. The observed precipitation and temperature data are obtained from the IMD and wind speed data from Climate Forecast System Reanalysis (CFSR). All these data are brought to a grid resolution of 0.5° at which the model is implemented. The observed streamflow at monthly scales for two stations: Bhimagodha and Ankinghat are obtained from the CWC for validation of the simulated discharge. The regulated flow is converted to naturalized flow by incorporating the data pertaining to the water control/ diversion structure. In the upstream of the Ankinghat gauge station, water is diverted from the main Ganga River by diversion structures viz. Upper Ganga Canal, East Ganga Canal, Madhya Ganga Canal, East Ganga Canal and Lower Ganga Canal. The data corresponding to the canals were obtained from the CWC and added to the monthly discharge at Ankinghat gauge station, in order to convert the regulated streamflow to naturalised streamflow. The same methodology was also used in Chawla and Mujumdar (2015). For further understanding, an example of monthly discharge calculation for the year 2000 is given (Table S1). The satellite based soil moisture data, used for validation, is a merged product from European Space Agency Climate Change Initiative (ESA CCI), which is at a spatial resolution of 0.25° and temporal resolution of daily scale, for the period of 1978–2005. The simulated ET is validated using the Moderate Resolution Imaging Spectroradiometer (MODIS) MOD16 Global Terrestrial Evapotranspiration Data Set, which is at monthly time scale and at a spatial resolution of 1 km. It is available for a period of 2000–2010. The in-situ soil moisture for two stations viz. KRN and KLNI at a 7 day interval during the monsoon season was procured from IMD.

2.4. Monte Carlo simulations

MCS is a method of translating the uncertainty in the model inputs parameters to the model output. Probability distributions for the inputs parameters are assumed and random samples are generated which are utilized to execute the model. Complex systems can be easily described through MCS even though being computationally very expensive and time consuming. Monte Carlo method has a wide variety of application including sensitivity analysis of hydrological models and uncertainty assessments. Demaria et al. (2007) used the Monte Carlo approach to study the sensitivity and identifiability of parameters controlling surface and sub-surface flow. Wilby (2005) used the Monte Carlo sampling approach in the historic climate variability context, to understand parameters stability and identifiability. MCS, to represent uncertainties, were also used by New and Hulme (2000) and Prudhomme et al. (2002).

In our study we assume that the sensitive soil parameters described in section 2.3.1 to follow triangular distribution with base being the prescribed range and mode being the recommended value (http://www.hydro.washington.edu/Lettenmaier/Models/VIC/Datasets/Datasets.shtml). The vegetation parameters are assumed to follow uniform distribution with a range of ± 0.1 times the prescribed value. The reason for choosing a range of ± 0.1 times the prescribed value is completely arbitrary and is one of the drawback of present study. Assuming these distributions, 1000 random numbers are generated for each of these sensitive parameters and the model is executed considering these set of generated parameters. These simulations are first performed for the observed period to evaluate the performance of the model. For climate projections, we executed these simulations for 4 sets of meteorological forcings which include statistically and dynamically downscaled products of 2 GCMs (IPSL and EC-EARTH). The results and interpretations of the simulations using Monte Carlo method are described in the following section.

3. Results and discussions

3.1. Model performance

The discharge data procured from Central Water Commission (CWC) for the two stations- Ankinghat and Bhimagodha are for a period of 1977–2009 and 1990–2011 respectively. Further to this, the MODIS ET data covers a time period of 2000–2010. Hence, a common period of 10 years i.e. 2000–2009 was selected for validation and the results are shown in Fig. 2. River routing is performed for the two stations-Bhimagodha and Ankinghat which are located in the Upper Ganga Basin, as shown in Fig. 1a. Time series of monthly discharge, as obtained from the observed data and from simulations performed 1000 times under

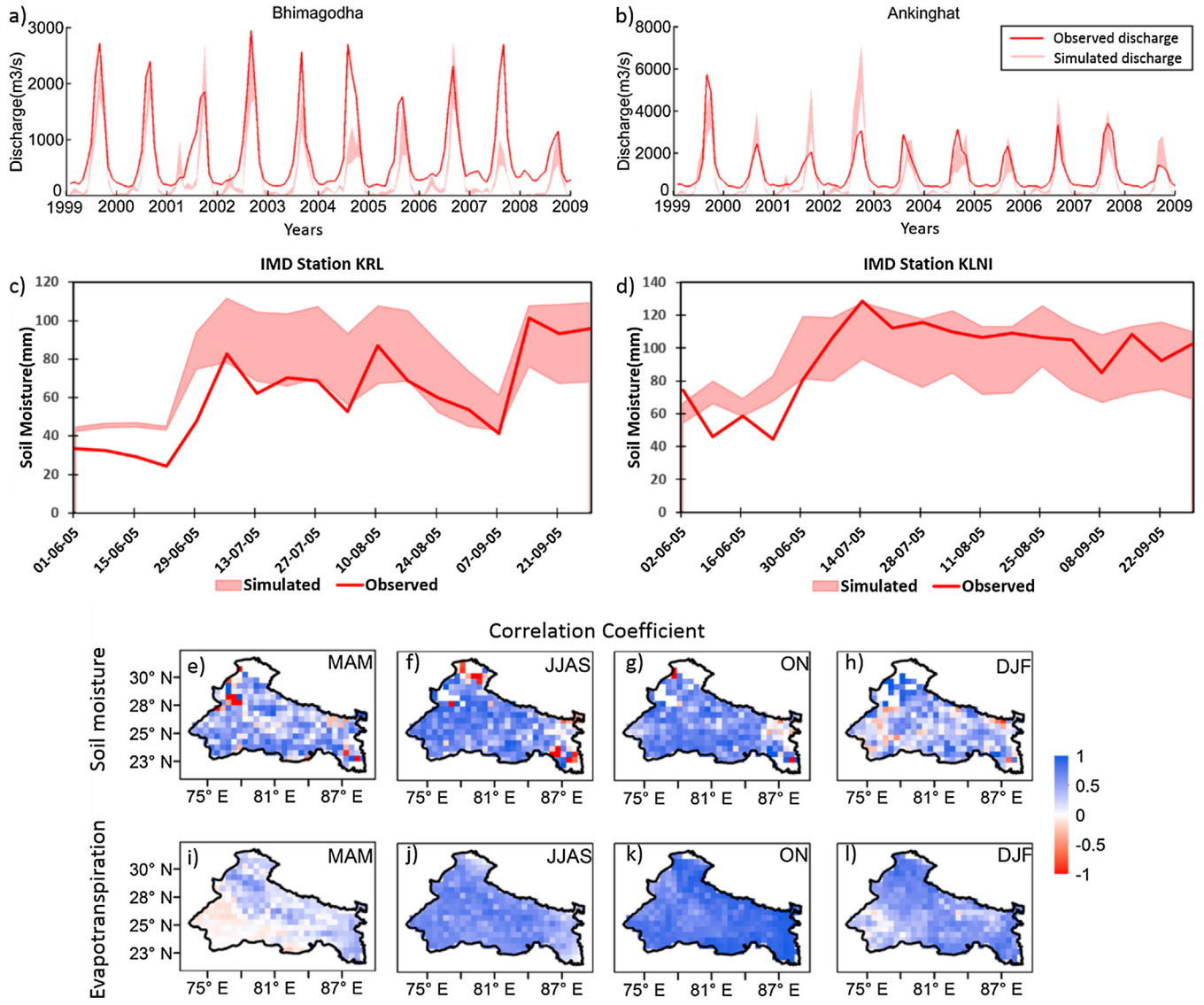

Fig. 2. Evaluation of VIC model outputs over the Ganga basin. The time series of observed and simulated monthly discharge at Bhimagodha (a), and Ankinghat (b) gauging stations are shown. The simulated soil moisture and in-situ observed soil moisture at KRN(c) and KLNI (d) IMD stations are presented. The band of simulated discharge and soil moisture are obtained by performing Monte–Carlo Simulations with the sensitive model parameters. Seasonal average of correlation coefficients between observed and ensemble mean of simulated soil moisture (d–g) and evapotranspiration (h–k) are presented.

the Monte Carlo scheme, at these two stations are presented in Fig. 2 a and b. For the simulated discharge, the band shows the uncertainty range and line shows the observed time series. The pattern of the observed discharge, especially the rising and the recession limbs are well captured by the simulations although the peaks do not match at Bhimagodha station. The error in modelling the extreme precipitation is a possible reason for the discrepancies in simulated peaks of streamflow. Here, the fact to be highlighted is that the basin under consideration is highly human intervened and the observed streamflow is controlled by reservoirs and dams. We also find negative bias in the low flow conditions which attributes to the groundwater contributions to the baseflow, which is not considered in VIC (Chawla and Mujumdar, 2015). The surface fluxes are greatly influenced by the groundwater interactions with an exception in case of arid regions where the groundwater can be disconnected (Rosenberg et al., 2013). The groundwater gets recharged during the wetter periods and contributes to the streamflow during the drier periods. In the Indian scenario, during the low flow period (November to May), groundwater is the key supplier to streamflow (Chawla and Mujumdar, 2015). Since the groundwater interactions are not considered, the model fails in reproducing the streamflow during the low-flow conditions. Moreover, same mismatches were observed in the study by Chawla and Mujumdar (2015). The simulated soil moisture was compared with the in-situ soil moisture available from IMD for 7-day interval during monsoon season. In Fig. 2(c) and (d), the band shows the range of simulated soil moisture and the line represents the observed soil moisture, both at a depth of 30 cm during June-September 2005, for two stations viz. KRL and KLNI. The pattern of the soil moisture is well captured by the model at the both stations. The performance of the hydrological simulations is also evaluated with the correlation coefficients between observed and simulated soil moisture and evapotranspiration. The observed and simulated values show good correlation with coefficients in the range of 0.7–0.9 during the monsoon and post-monsoon season, for both soil moisture and ET (Fig. 2(f), (g), (j) and (k)). The poor correlation coefficients in the other two seasons probably attribute to the non-consideration of ground water contribution (Fig. 2(e), (h), (i) and (l)). The groundwater dynamics influences the soil moisture, which in due course affects the water and energy fluxes between land and atmosphere (Fan et al., 2007). The coupling of VIC with groundwater model by Liang (2003) resulted in drier soil moisture in the top layers and

Table 3
Model performance statistics in terms of Nash Sutcliffe Efficiency (NSE), correlation coefficient (R) , Root Mean Square Error (RMSE) and refined index of agreement (d_r)with respect to discharge, soil moisture (SM) and evapotranspiration (ET) at Ankinghat and Bhimagodha.

Station Name	NSE	Parameters						R discharge	RMSE	dr	R ET				R SM			
		Dsmax	Ds	Ws	binf	d2(m)	d3(m)				MAM	JJAS	ON	DJF	MAM	JJAS	ON	DJF
Ankinghat																		
NSE(max)	0.63	29.2	0.98	0.98	0.39	2.5	1.46	0.84	630.36	0.69	0.08	0.45	0.8	0.32	0.65	0.83	0.5	0.94
NSE(min)	0.26	1.93	0.11	0.1	0.04	0.43	0.16	0.85	670.15	0.62	0.07	0.38	0.88	0.25	0.63	0.82	0.62	0.93
Bhimagodha																		
NSE(max)	0.64	29.8	0.72	0.78	0.32	2.36	1.06	0.83	437.9	0.7	0.07	0.52	0.88	0.67	0.81	0.68	0.77	0.86
NSE(min)	0.34	6.67	0.07	0.11	0.04	0.43	0.16	0.84	523.77	0.64	0.14	0.59	0.89	0.45	0.75	0.71	0.71	0.83

lesser evapotranspiration in comparison to default VIC. Thus, the non-consideration of groundwater in the model contributes to the bias in estimated soil moisture and evapotranspiration. We have calculated the model performance statistics: Nash Sutcliffe efficiency (NSE), Correlation Coefficient (R), root mean square error (RMSE) and refined index of agreement (d_r) (Willmott et al., 2012) considering river discharge, soil moisture and ET for each of the simulations and depicted the extreme cases in Table 3. We find that, when, NSE shows lowest value for streamflow its performance is better for other variables as compared to that corresponding to highest NSE of streamflow. This necessitates the use of all hydrologic variables, rather than focussing only on streamflow. This further explains the reason behind non-removal of any of the simulations from uncertainty estimation. Further to this, the non-regulated streamflow is only available for Upper Ganga Basin. Hence, we cannot calibrate the model for entire Ganges with the same data. Considering these facts, we allow the model parameters to freely take any values to get a better picture of uncertainty. A considerable area of the basin is cropland with intensive irrigation (Fig. 1(b)). Hence, the other reason behind poor correlation could be the non-consideration of irrigation in VIC model. The seasonal mean of the VIC simulated evapotranspiration also shows good resemblance with MODIS-ET in all seasons except monsoon (Fig. 3a–h). During the monsoon season, there is a high discrepancy between the simulated and MODIS ET. It should be noted that the cloud cover is very high during monsoon and that may lead to an erroneous ET data from satellite the MODIS products. The mismatch may attribute to the quality of observed remote-sensing datasets. We find a good resemblance in the shape of climatological ET between MODIS and simulated data, though the simulated data overestimates the same (Fig. 3i). For further investigation, we plot ET from CFSR, Interim ECMWF Re-Analysis (ERA-interim) and Modern Era-Retrospective Analysis (MERRA) and find a consistent underestimation of ET by MODIS. Inaccuracies in the ET from MODIS due to over or underestimation has been reported in other studies (Kim et al., 2012; Ramoelo et al., 2014). The satellite observed soil moisture data acquired from ESA CCI covers a depth of 0.5–2 cm. The depth of the top layer in our model is 0.3 m and hence comparing it with satellite soil moisture will have its own limitations. We have made the assumption that the soil moisture is uniformly distributed over the top layer and calculated the soil moisture at a depth of 2 cm, for the purpose of calculating the correlation coefficient. The resampling of the data to the spatial resolution of the model was done using the method of bilinear interpolation. The spatial plots of mean observed and simulated soil moisture, following the same methodology, is plotted for all the four seasons of the year (Fig. 4). It is observed that the spatial pattern soil moisture is captured well by the model for different seasons but with non-uniform biases

3.2. Future projections

The spatial pattern of the mean of accumulated precipitation over various seasons, for each GCM-downscaling combination with that of IMD observed data is compared in Fig. 5. It can be observed that the overall spatial pattern is captured well by the downscaled models with a few exceptions. All the models perform well during monsoon and winter season. However, during the pre-monsoon and post-monsoon, EC-Earth CORDEX and IPSL CORDEX output tend to overestimate precipitation over the upper and middle reaches of the basin. Small changes in temperature or precipitation can cause an amplified impact on the components of water cycle (Milly et al., 2005). Therefore, we compare the spatial pattern of seasonal changes in precipitation and temperature from each of the GCM-downscaling combination in Figs. 6 and 7, respectively. EC-EARTH CORDEX, IPSL CORDEX and MPI CORDEX represent the dynamic downscaled output of EC-EARTH, IPSL and MPI respectively; whereas, EC-EARTH SD, IPSL SD and MPI SD represents the corresponding statistical downscaled product. Each row in Fig. 6 represents mean of changes in precipitation between the periods of 2011–2037 and 1979–2005 for each of the seasons- pre-monsoon (MAM), monsoon (JJAS), post-monsoon (ON) and winter (DJF) and columns indicate different GCM-downscaling combinations. Similar sequence is followed for maximum and minimum temperature in Fig. 7. During the pre-monsoon, all the projections except that corresponding to IPSL show moderate increase in precipitation over most of the regions. Few regions are observed to have no change in the projected precipitation. In the lower Ganga Basin, very high increment of pre-monsoon precipitation can be observed for EC-EARTH CORDEX, IPSL CORDEX and MPI SD. We observe a decline in precipitation in the upper and middle Ganga for IPSL CORDEX. During the monsoon season, we find a mild to moderate increase in precipitation at most of the places in the basin, except in case of MPI products. A decline in precipitation can be observed in upper Ganga Basin for MPI CORDEX and MPI SD, the decline being more pronounced in case of the latter. However, there is a high increase in monsoon precipitation in the middle and lower reaches of the basin for MPI SD simulation. EC-EARTH CORDEX and EC-EARTH SD show an increase in precipitation during the post monsoon season. IPSL CORDEX and MPI SD show exactly opposite change. The six simulations provide six entirely different precipitation scenarios of winter precipitation. It is important to note that for other seasons, there is occasional agreement in large scale trends; however the spatial patterns are almost entirely different across different model runs for all the seasons. Similarly, the maximum temperature also shows variations in the spatial pattern for each season. All the projections for maximum temperature show increase, the magnitude being more for IPSL-SD, MPI CORDEX and MPI SD (1.2–1.6°). During winter, EC-EARTH CORDEX, MPI CORDEX and MPI SD show very high increase in maximum temperature. Similar results are obtained for minimum temperature; EC-EARTH SD and MPI SD showing maximum increase during the post monsoon and winter respectively. It can be noted that during monsoon season, the projections of maximum temperature from multiple GCM-downscaling combinations have higher agreements. Overall, it is evident that there are high discrepancies across GCMs and downscaling models for the precipitation and temperature projections during all the seasons. We also plotted the trends in the precipitation, maximum and minimum temperature in the Figs. 8–10 respectively. In Fig. 8a, the trend across the 3 GCMs are

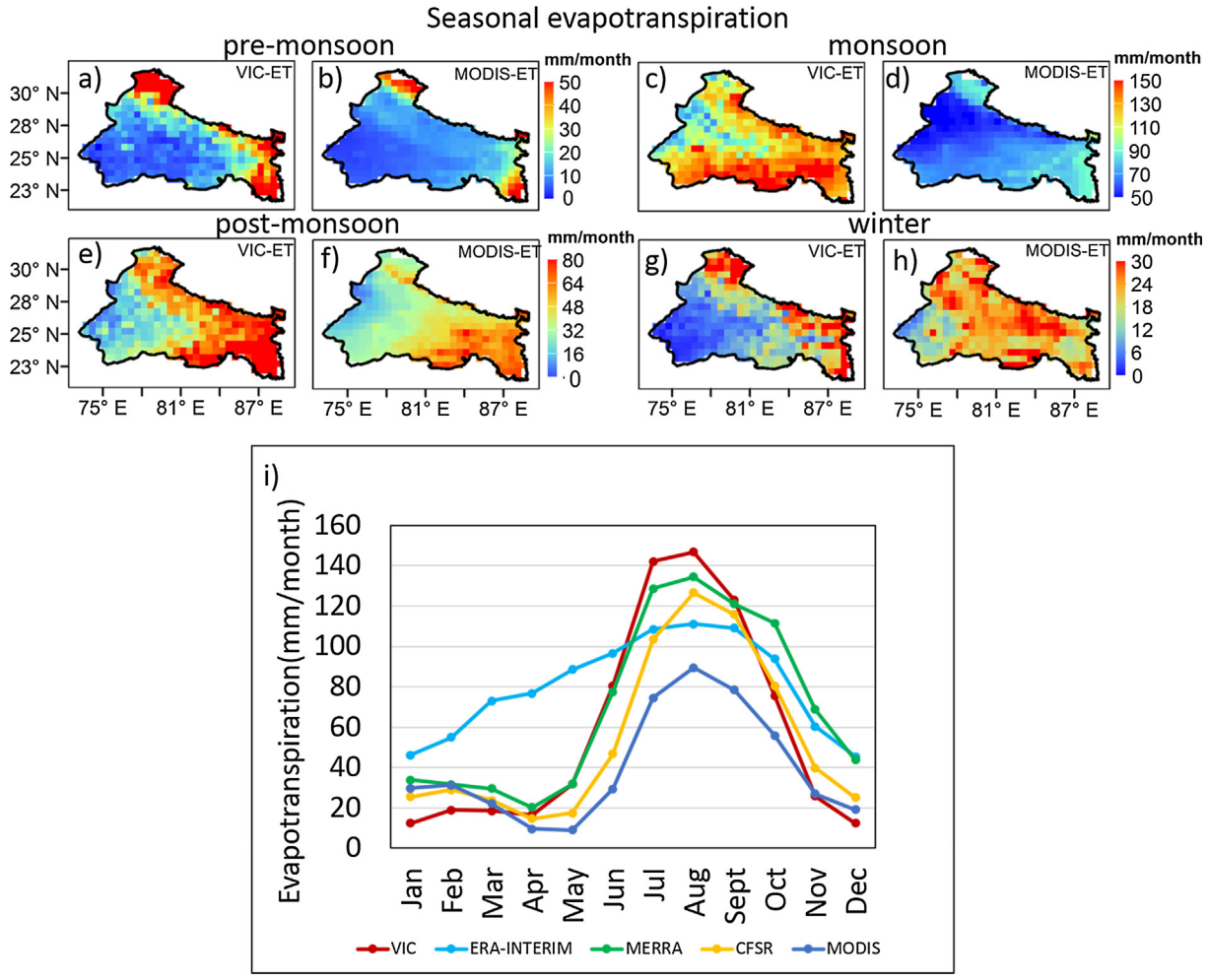

Fig. 3. Mean seasonal MODIS–ET (b, d, f, h) and mean seasonal VIC–simulated–ET (a, c, e, g). Here, VIC–simulated–ET represents mean of ET values obtained from various combinations (ensemble) of the hydrological model parameters. The seasonal ET values obtained from MODIS–ET, and VIC–simulated–ET show similar pattern during the pre–monsoon and post monsoon seasons. Climatologies of ET from VIC, ERA–Interim, MERRA, CFSR, and MODIS are presented in (i).

considered with the band representing the uncertainty due to downscaling. The precipitation trend across different downscaling techniques (statistical and dynamical downscaling) is represented in Fig. 8b, the band depicting the uncertainty across GCMs. In Fig. 8c, the trend in precipitation across the 3 GCMs and 2 downscaling techniques is shown. In general, the future precipitation is observed to decrease. The peaks in the precipitation is sharper for the future scenarios. The maximum and minimum temperatures show increasing trend in future (Figs. 9 and 10). As expected, the uncertainty due to the downscaling technique is less as compared to the GCM uncertainty.

The uncertainty arising from multiple GCMs, when they are used in statistical downscaling is explained by calculating the partial correlation of the predictors involved in statistical downscaling with respect to the predictands for all the GCMs (Table 4). It can be observed that the values of the partial correlation has wide range of variation among the GCMs during all seasons, with inconsistencies even in signs. The surface

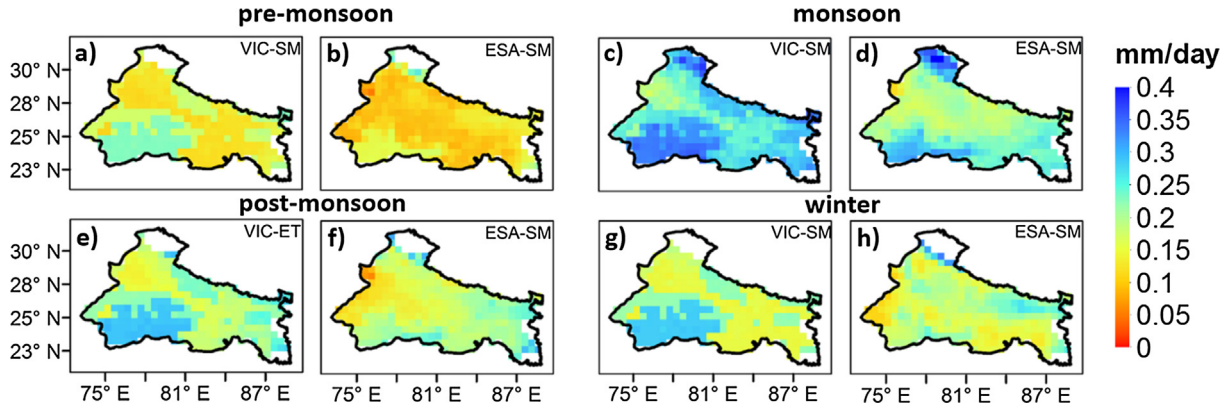

Fig. 4. Mean seasonal ESA-SM (b, d, f, h) and mean seasonal VIC–simulated–SM (a, c, e, g). Here, VIC–simulated–SM represents mean of SM values obtained from various combinations (ensemble) of the hydrological model parameters.

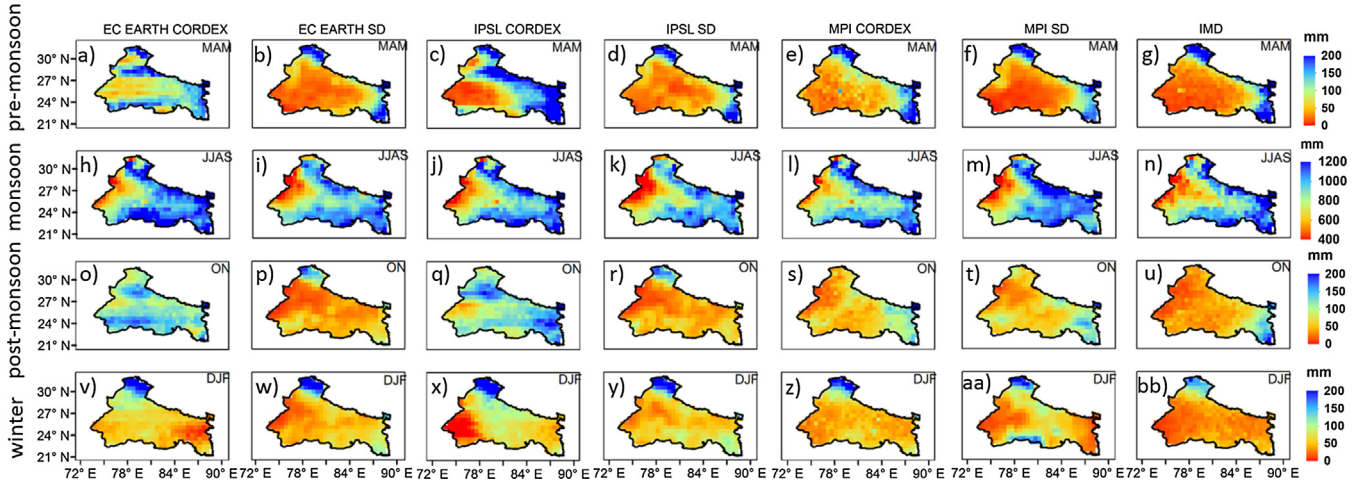

Fig. 5. Mean accumulated precipitation over various seasons during the period of 1979–2005 simulated by EC–EARTH CORDEX (a, h, o, v), EC–EARTH statistical downscaling [(EC–EARTH SD),(b, i, p, w)], IPSL CORDEX (c, j, q, x), IPSL statistical downscaling [(IPSL SD), (d, k, r, y)], MPI CORDEX(e, l, s, z) and MPI statistical downscaling [(MPI SD), (f, m, t, aa)] compared with IMD observed data (g, n, u, bb).

humidity shows a positive correlation for all the GCMs during the past and future; the values have a wide range across GCMs (with negative values during some of the seasons) and this results into uncertainty in the projections of precipitation. Similarly, the sea level pressure shows a wide variation in the correlation values, even though it is mostly negative. During the past, the partial correlation value for temperature at 500 hPa are not consistent even with the signs. Similar is the case with surface u-wind and v-wind at 500 hPa during both past and future. The other predictors also show a wide variations in the partial correlation. From the above observations, it can be concluded that the relation between predictors and predictand is different across different GCMs even when the same downscaling is applied and this results into very high uncertainty in the projections.

3.3. Uncertainty in hydrologic projection

Hydrologic modeling is performed with VIC for the historical simulations and future projections, using the meteorological data as obtained for different GCMs and downscaling combinations. MCS are performed to assess the uncertainty in river discharge. The simulated changes in discharge for future (2011–2037) with respect to the past (1979–2005), corresponding to each of the 1000 sets of simulations, during each season are represented in Fig. 11 with the help of box plots. Each of the box plot corresponds to the output for the six meteorological forcing sets. The width of each of the box plots denotes the spread of the projected changes resulting from 1000 simulations corresponding to a specific GCM-downscaling combination, and hence it quantifies the hydrologic parameter uncertainty. The differences between two box plots show the climate model uncertainty. From Fig. 11, it is clearly visible that the range of variation in discharge due to parameter uncertainty is very less when compared to the climate model uncertainty. The width of box plots for all the cases look almost insignificant as compared to the differences in positions between the boxes. There is also no overlap between the boxes showing very high uncertainty resulting from the use of multiple climate models for all the seasons. For example, during the pre-monsoon season, where the dynamic downscaled product of all the three GCMs show decrease in the streamflow, the statistical downscaled products show increase in the

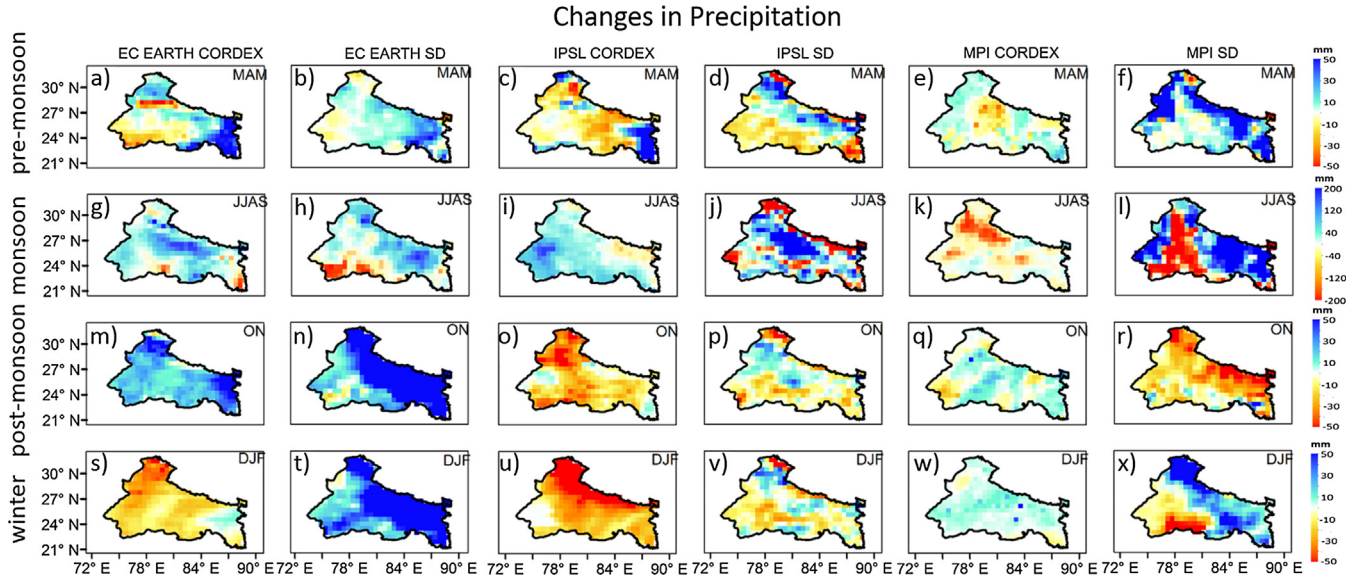

Fig. 6. Seasonal average of changes in precipitation between the period of 2011–2037 and 1979–2005 simulated by EC–EARTH CORDEX (a, g, m, s), EC–EARTH statistical downscaling [(EC–EARTH SD),(b, h, n, t)], IPSL CORDEX (c, i, o, u), IPSL statistical downscaling [(IPSL SD), (d, j, p, v)], MPI CORDEX(e, k, q, w) and MPI statistical downscaling [(MPI SD), (f, l, r, x)].

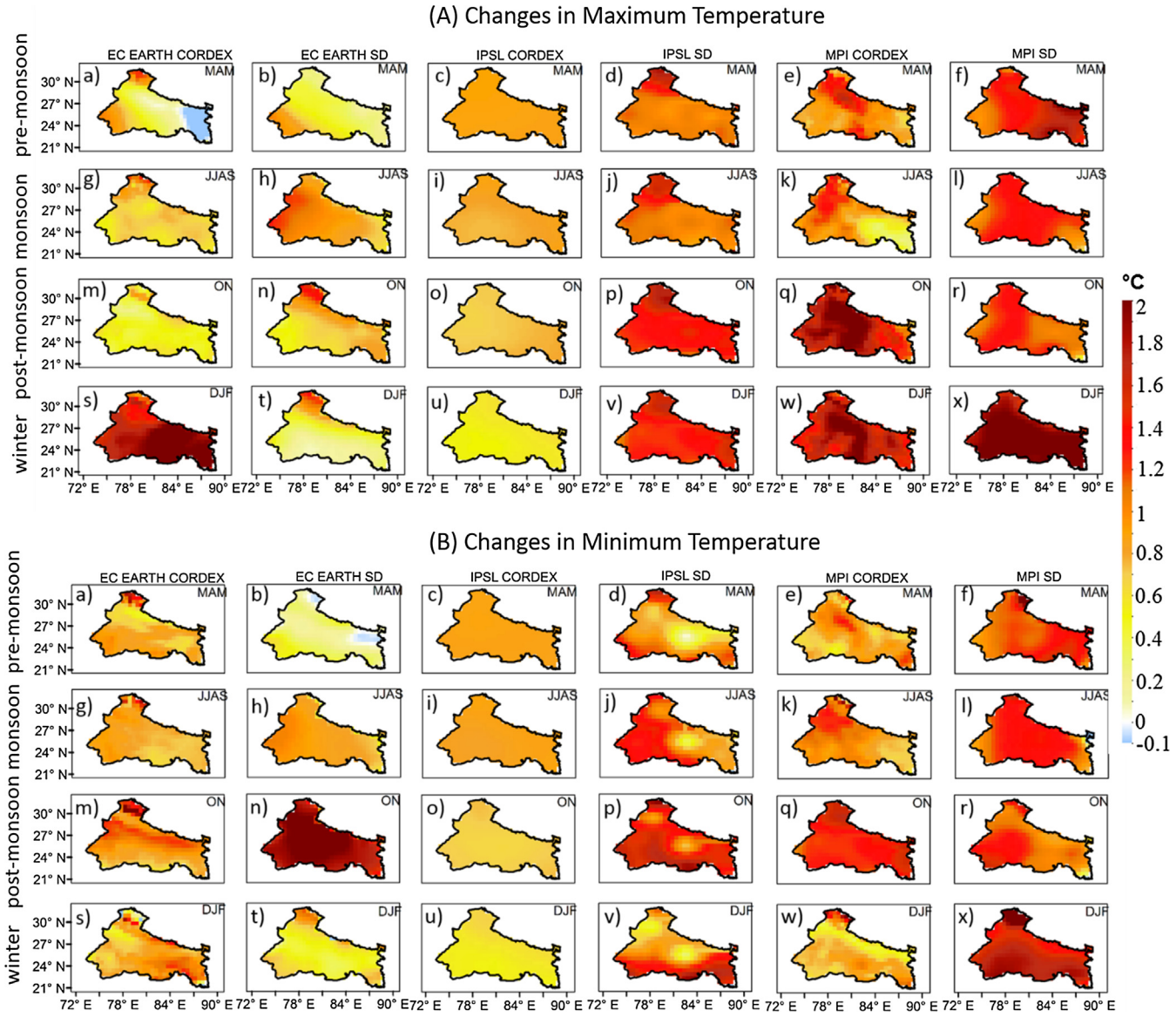

Fig. 7. Seasonal average of changes in (A) maximum temperature (B) minimum temperature between the period of 2011–2037 and 1979–2005 simulated by EC–EARTH CORDEX, EC–EARTH statistical downscaling (EC–EARTH SD), IPSL CORDEX, IPSL statistical downscaling (IPSL SD), MPI CORDEX and MPI statistical downscaling (MPI SD).

same. The differences across models are not just in terms of values but also in terms of the signs in changes. Such a huge uncertainty provides very little confidence to the policy makers to use the projections for water management in adapting to climate change. If we consider the individual simulation, the changes in precipitation and temperature are reflected well in the simulated streamflow at the two stations. For the pre-monsoon season, the impacts of increase in the precipitation is prominent in the streamflow for IPSL SD and MPI SD. Streamflow corresponding to all the CORDEX simulations show prominent decrease which is attributed to the decline in precipitation. In monsoon season, there is an overall increase in streamflow for Ankinghat, in exception to that corresponding to both the MPI products, which is very similar to the changes in precipitation in the upper to middle Ganga Basin. On the other hand, at Bhimagodha, the simulated streamflow from IPSL SD and MPI CORDEX show a decline due to reduced precipitation as well as increase in temperature at the upper reaches of the basin. During the post monsoon and winter season, the pattern of changes in the streamflow is clearly driven by precipitation. We observe that the simulated streamflow from EC-EARTH SD has the maximum increase and that from IPSL CORDEX shows a decrease, which is analogous to their corresponding precipitation pattern. Also, large differences in changes in simulated river discharge across the statistical and dynamically downscaled data is observed, that can be attributed to the difference in the projected precipitation. The changes in discharge for EC EARTH during the post monsoon and winter show huge differences between the statistical and dynamically downscaled data, which is analogous to the precipitation pattern. During the post monsoon season, upper reaches of the Ganga Basin show an increase in precipitation of more than 50 mm for EC EARTH SD. On the other hand, precipitation increase corresponding to EC EARTH CORDEX is in the range of 10–30 mm, with a few grids showing an increase of 50 mm. Winter precipitation is also found to have large uncertainty across the EC EARTH CORDEX and EC EARTH SD (-30 mm and 50 mm respectively). Hence, it can be concluded that the huge difference in precipitation is the reason for the differences in the river discharge.

We further demonstrate and compare the uncertainties in terms of the Probability Density Functions (pdfs) of hydrologic variables representing their spatial variability across the basin. The spatial pdfs for the changes in evapotranspiration and soil moisture are shown in Fig. 12 with the band representing the parameter uncertainty and

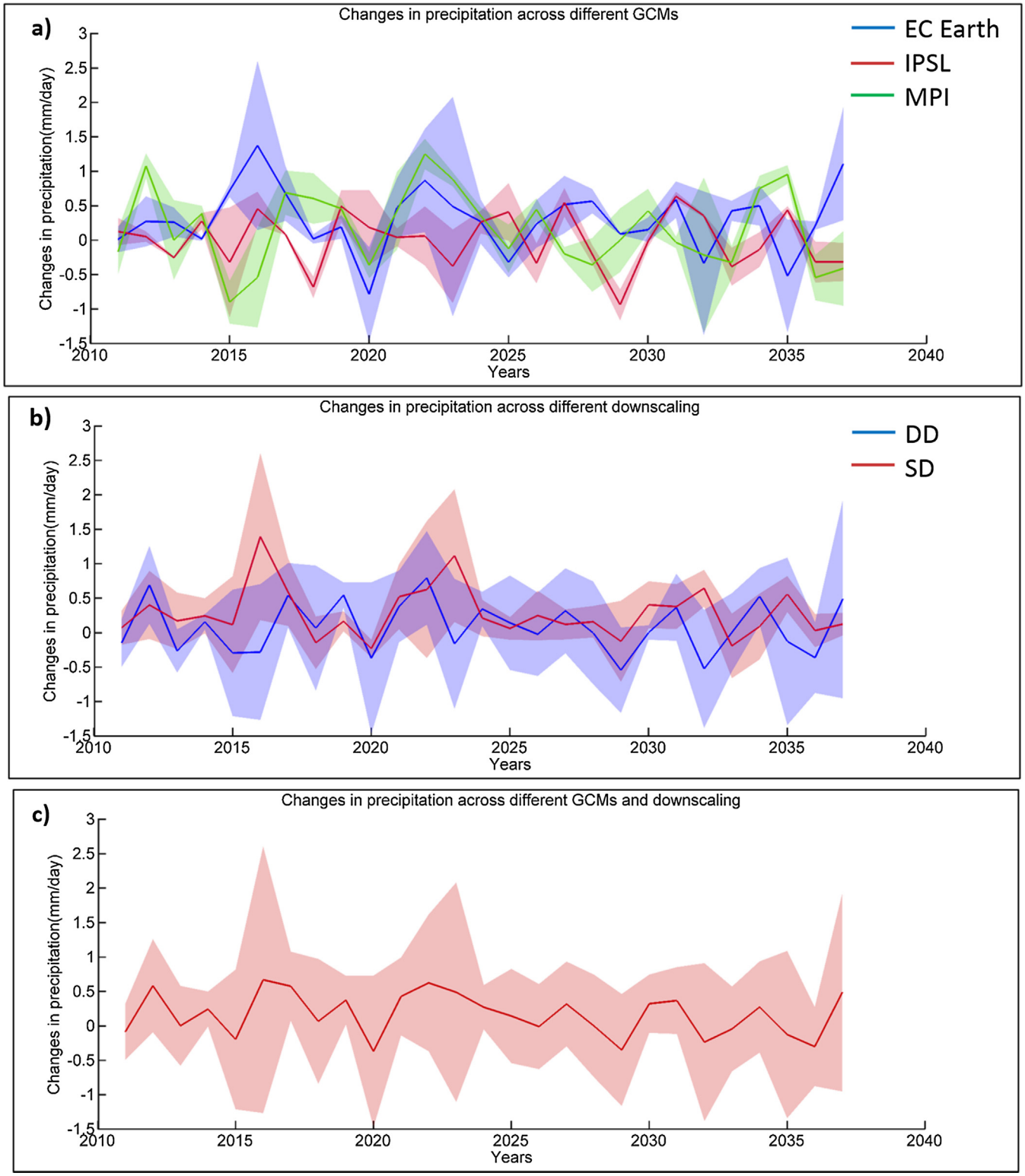

Fig. 8. Trends in changes in precipitation across different GCMs (a), downscaling (b) and GCMs and downscaling (c).

different colors showing the 6 GCM-downscaling combinations. The widths of the bands are very less when we compare them with the differences between the pdfs of different colors. This further strengthens our conclusion that the parameter uncertainty is less, compared to multi-climate model uncertainty. We also observe that the width of the band of pdf presenting the projected changes in ET during monsoon is less than that of soil moisture. The parameters like Ds, Dsmax and Ws are involved in the non-linear formulation of the baseflow at the time of its rapid generation during extreme wet condition (Raje et al., 2014). Hence, they are more sensitive to the soil moisture during the same season resulting an increase in uncertainty associated with their parameterization. Similarly, the parameters sensitive to evapotranspiration (vegetation parameters) are activated during the dry season due to the limited supply of moisture to the plants.

Fig. 13 represents box plots for changes in the total water yield, i.e.,

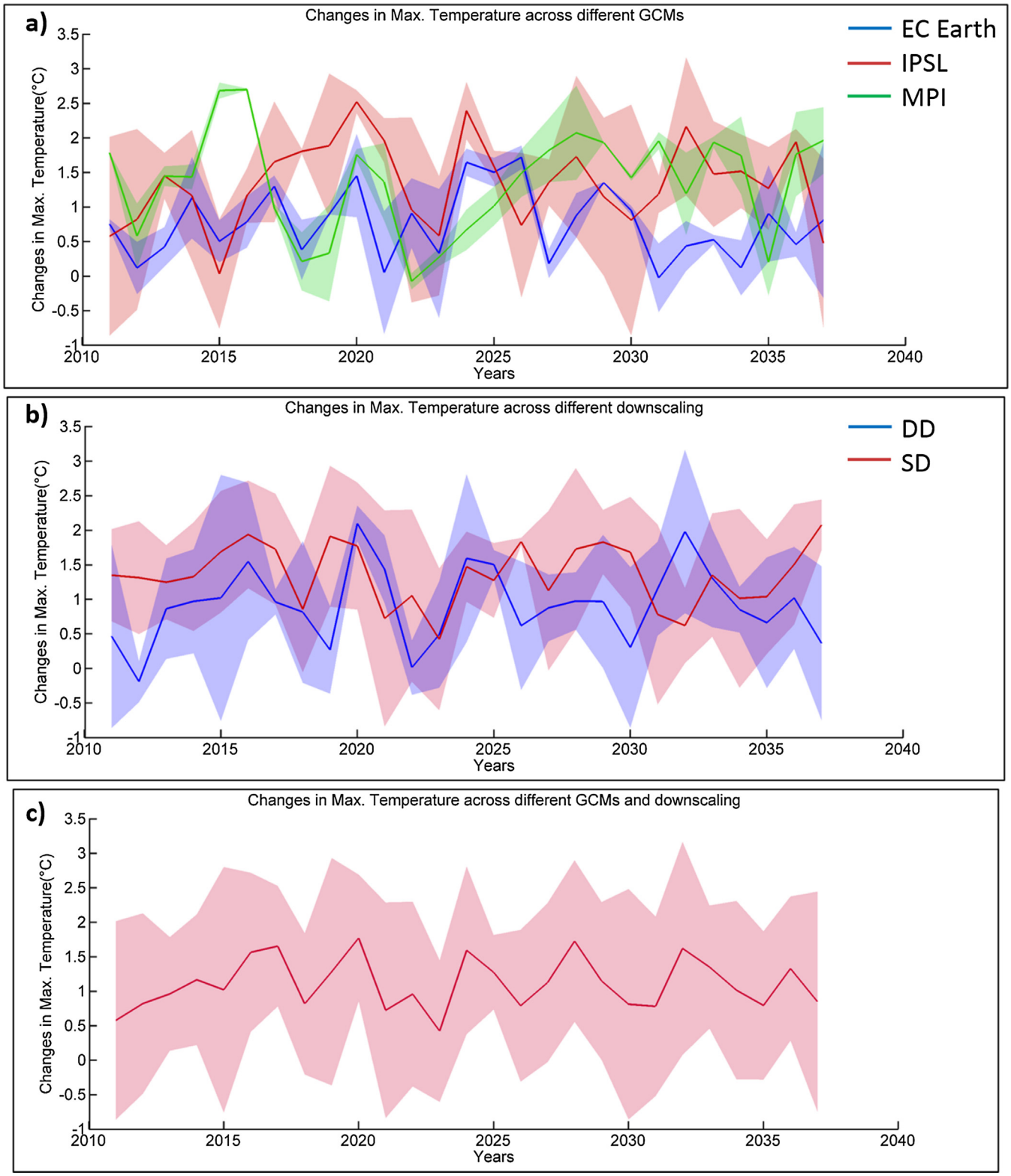

Fig. 9. Trends in changes in maximum temperature across different GCMs (a), downscaling (b) and GCMs and downscaling (c).

sum of baseflow and runoff (Ghosh et al., 2016), for future (2011–2037) with respect to the past (1979–2005) averaged over each of the four seasons plotted separately for upper, middle as well as lower Ganga Basin (Koshal, 2014). The spread of the projected changes resulting from 1000 simulations corresponding to a specific GCM-downscaling combination, is represented by the width of each box plot. Similar to Fig. 11, it is observed in Fig. 13, that the width of box plot representing the hydrological parameter uncertainty is very less compared to the distance in positions between the boxes and this further supports the inference from the previous figures. The water yield corresponding to EC-EARTH CORDEX shows a decrease during pre-monsoon season over the upper and middle Ganga Basin. During monsoon and post monsoon, we observe increase in water yield for all the regions of the basin. However, during the winter season, decreased water yields are

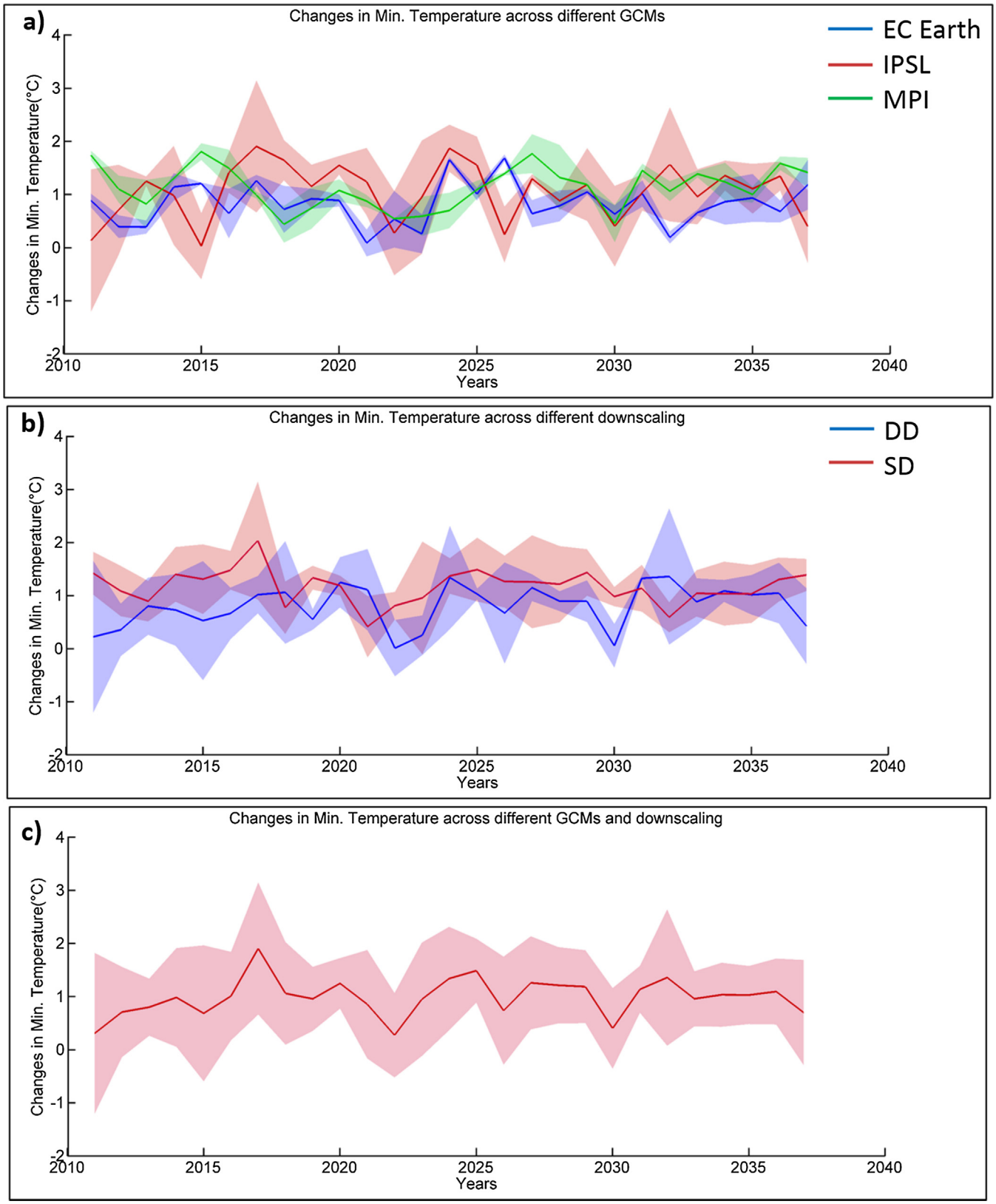

Fig. 10. Trends in changes in minimum temperature across different GCMs (a), downscaling (b) and GCMs and downscaling (c).

projected for upper and middle Ganga Basin. For the simulations from EC-EARTH SD, during the pre-monsoon season, decreased water yield is projected for upper Ganga, increased water yield is projected for middle Ganga and no change is observed for lower Ganga Basin. During other seasons, increased water yields are projected over all the regions of the basin. The water yield corresponding to IPSL CORDEX is projected to increase during the pre-monsoon and monsoon season for upper and lower Ganga Basin. There is a widespread decrease in the water yield for IPSL CORDEX during the post-monsoon and winter season over the upper and middle Ganga Basin. The water yield corresponding to IPSL

Table 4
Partial correlation of predictors with the statistically downscaled precipitation.

	hus	psl	ta500	tas	uas	u500	vas	v500
EC_sd_past								
MAM	0.268	-0.022	-0.013	-0.202	-0.029	-0.031	0.197	-0.037
JJAS	0.020	0.089	0.115	-0.233	0.130	-0.123	0.237	-0.071
ON	-0.034	-0.033	0.006	0.030	-0.016	0.044	0.050	-0.021
DJF	0.104	-0.008	0.018	-0.166	0.095	-0.080	0.116	0.024
IPSL_sd_past								
MAM	0.478	-0.143	-0.036	-0.309	-0.083	-0.047	0.113	0.027
JJAS	0.226	-0.068	-0.020	-0.031	0.060	-0.025	0.131	-0.017
ON	0.068	0.057	-0.032	0.007	0.033	-0.011	0.011	-0.042
DJF	0.083	-0.022	-0.041	-0.089	0.010	-0.070	0.054	0.037
MPI_sd_past								
MAM	0.269	-0.200	-0.040	-0.219	-0.143	-0.036	0.021	0.035
JJAS	0.102	-0.145	0.065	-0.221	0.079	-0.095	0.247	0.000
ON	0.266	-0.152	0.109	-0.317	-0.028	-0.090	0.187	0.062
DJF	0.054	0.033	0.006	-0.017	0.044	-0.027	-0.001	0.005

	hus	psl	ta500	tas	uas	u500	vas	v500
EC_sd_future								
MAM	0.125	-0.004	0.071	-0.152	-0.017	-0.017	0.038	-0.012
JJAS	0.089	0.153	0.080	-0.156	0.097	-0.032	0.037	0.003
ON	0.142	-0.009	0.097	-0.122	-0.027	0.032	0.038	-0.057
DJF	0.080	-0.068	0.091	-0.163	0.034	-0.088	0.002	-0.021
IPSL_sd_future								
MAM	0.405	-0.183	-0.054	-0.228	-0.092	-0.040	0.106	0.020
JJAS	0.233	-0.022	-0.040	-0.062	0.087	-0.023	0.158	0.014
ON	-0.040	-0.006	0.048	0.014	-0.035	0.027	0.007	0.012
DJF	0.073	-0.004	0.021	-0.085	0.024	-0.052	0.045	0.016
MPI_sd_future								
MAM	0.058	-0.105	0.021	0.104	-0.093	0.066	-0.055	-0.002
JJAS	0.080	-0.014	0.057	0.008	0.004	-0.004	0.038	-0.013
ON	-0.015	-0.089	-0.025	0.091	-0.015	0.034	-0.047	-0.051
DJF	-0.017	0.031	0.001	0.026	-0.043	0.080	0.006	-0.016

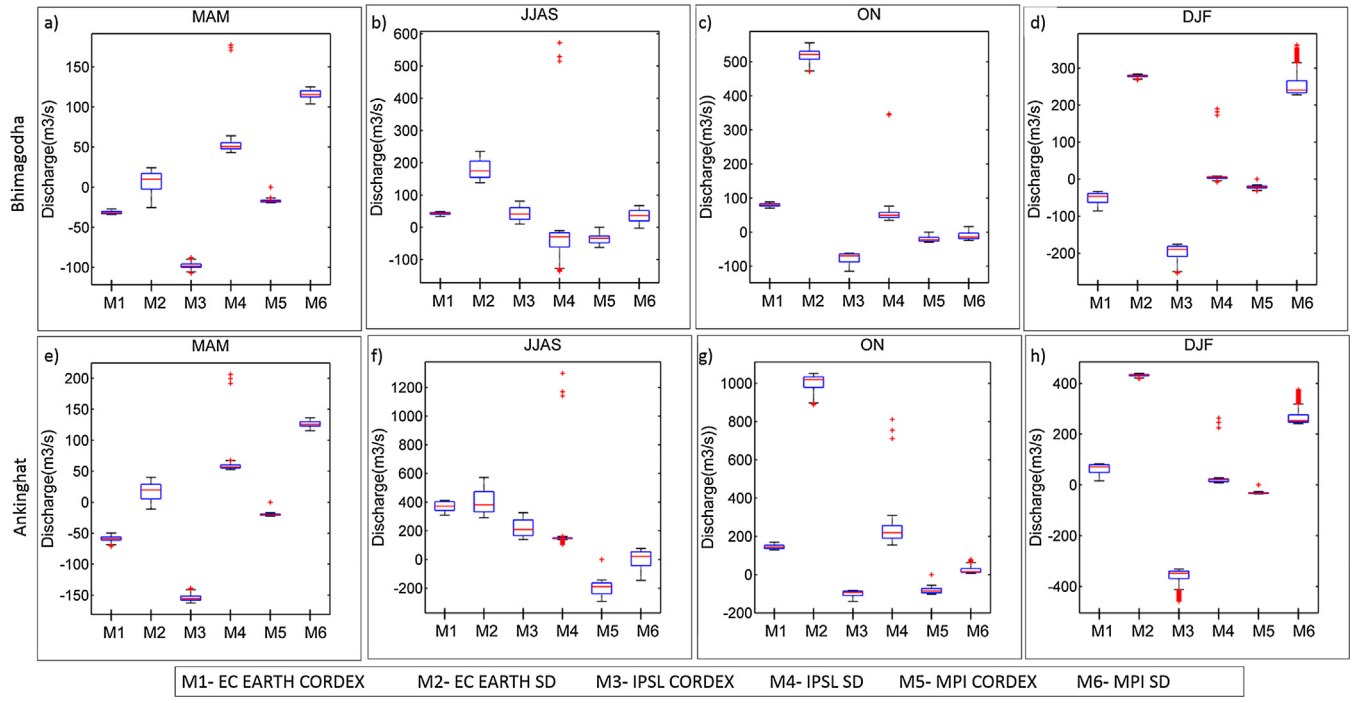

Fig. 11. Changes in the simulated monthly discharge (calculated using Monte–Carlo simulations), averaged over four seasons between the period of 2011–2037 and 1979–2005 for EC–EARTH CORDEX (M1), EC–EARTH statistical downscaling [(EC–EARTH), M2], IPSL CORDEX (M3), IPSL statistical downscaling [(IPSL SD), M4], MPI CORDEX (M5) and MPI statistical downscaling [(MPI SD), M6] at Bhimagodha (a–d) and Ankinghat (e–h) gauging stations. The widths of the box plots represent the hydrological model parameter uncertainty which is quite small compared to differences in simulations between climate models.

SD is projected to increase over all the regions during the all the seasons except post monsoon where there is a slight decrement in lower Ganga basin. An increment in the water yield is observed during the pre-monsoon season for MPI CORDEX over all the three regions. However during the monsoon season, there is a decline in water yield over the basin other than lower Ganga basin. We can observe a mild increase in the water yield for upper and lower Ganga basin during post monsoon season. In the middle Ganga basin, on the other hand, the water yield shows negligible change. During winter, there is widespread increment of water yield except over the lower Ganga basin. The water yield is projected to increase over all the three reaches of the basin throughout all the seasons for MPI SD.

Similar to Fig. 11, changes in temperature and precipitation are clearly exhibited by the changes in water yield (Fig. 13). The results are presented separately for upper, middle and lower Ganga basins.

a) Upper Ganga Basin

In the upper Ganga basin, which is a hilly region, the changes in water yield is dependent on both precipitation and temperature. The snowmelt contributes significantly to the water yield at the grids with higher altitude, especially during the pre-monsoon season, and hence temperature plays a vital role over those grids. During the pre-monsoon season, EC-EARTH CORDEX shows a decline in water yield, which is possibly due to the reduction in the precipitation in that region. The water yield corresponding to EC-EARTH SD is observed to have a mild decline which is attributed to the nearly negligible precipitation change. The water yields, as simulated by VIC, with meteorological inputs from IPSL CORDEX, IPSL SD, MPI CORDEX and MPI SD show an increase, with IPSL SD and MPI CORDEX being slightly higher. During the monsoon season the water yield, as projected for all the regions

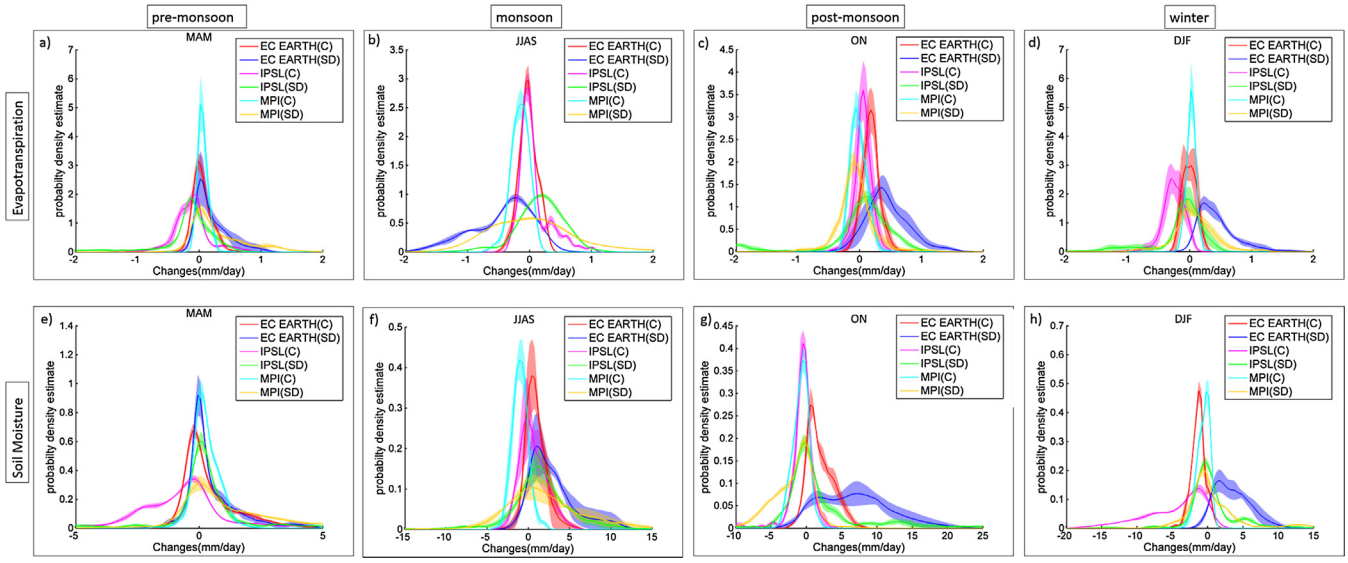

Fig. 12. Spatial probability density function for seasonal average of changes in evapotranspiration (a–d) and soil moisture (e–h) between 2011 and 2037 and 1979–2005 for EC–EARTH CORDEX (EC–EARTH C), EC–EARTH statistical downscaling (EC–EARTH SD), IPSL CORDEX (IPSL C), IPSL statistical downscaling (IPSL SD), MPI CORDEX (MPI C) and MPI statistical downscaling (MPI SD). Here, the band represents the uncertainty due to the sensitive hydrological parameters. The width of band is quite small compared to the differences in pdfs representing climate model uncertainty.

with all the combinations except MPI CORDEX, show an increase, with higher increment for EC-EARTH CORDEX and IPSL CORDEX over upper Ganga basin. Similar pattern is observed for the changes in precipitation. During the post monsoon season, an increase in water yield is generally observed except for IPSL CORDEX simulations, which is directly related to the changes in precipitation. The maximum increase in water yield is observed for simulations forced with EC-EARTH SD, which is similar to the changing precipitation pattern. During winter, it can be observed that the water yield simulated with EC-EARTH CORDEX and IPSL CORDEX outputs show decrease whereas the simulations using all the other GCM downscaling combinations show increase. The maximum increase in precipitation is projected for EC-EARTH SD and maximum decrease is for IPSL CORDEX, which is well reflected on the changes in water yield. The reduced precipitation projected by EC-EARTH CORDEX in upper reaches may be the reason for decreased water yield.

b) Middle Ganga Basin

As observed in upper Ganga basin, changes in precipitation is the major driving factor for variations in the water yield in the middle Ganga basin with a few exceptions. During pre-monsoon season, the water yield simulated with EC-EARTH CORDEX and IPSL CORDEX shows a reduction which is attributed to the corresponding decrease in precipitation. The projected precipitation from all other GCM-downscaling combination show increase which is reflected in the water yield changes. An overall increase in monsoon water yield can be observed in the middle Ganga basin except for the simulation corresponding to MPI CORDEX, which is attributed to the precipitation changes. Besides, it can be noted that the maximum increase in precipitation is observed for MPI SD which is reflected in the water yield changes. During the post monsoon season, the pattern of changes in water yield is analogous to the monsoon season with an exception of IPSL CORDEX simulated water yield. The changes in the precipitation is the major driving factor for this pattern. The water yield simulated using IPSL SD meteorological data depicts a marginal increase, following the corresponding pattern of changes in precipitation which include grids with mild increase/decrease. The reduced precipitation for IPSL CORDEX is captured well by the decline in corresponding simulated water yield. During the winter season, we observe that changes in water yield is highly dependent on the variations in precipitation. The water yield simulated with EC-EARTH CORDEX indicates a decrement, which is probably due to decreased precipitation and the projected increase in temperature causing more evaporation.

c) Lower Ganga Basin

In lower Ganga, there is an interplay between the changes in precipitation and temperature. During pre-monsoon season, EC-EARTH CORDEX shows an increase in water yield which is possibly due to the increment in precipitation. Water yield for EC-EARTH SD shows no change even though there is an increase in precipitation. This could be due to the slight increase in temperature. Since the lower Ganga is mostly flat terrain, the water yield is highly dependent on temperature and subsequently on evapotranspiration. Water yields simulated with the outputs of both downscaled products of MPI and IPSL show increase, IPSL CORDEX being greater during the pre-monsoon season. Similar pattern can be noticed in projected precipitation as well. During the monsoon season, increments in the simulated water yield attribute to increase in precipitation. During post monsoon season, the increase in precipitation is reflected in the increased water yield for EC-EARTH products. The projected precipitation during post monsoon by IPSL CORDEX and IPSL SD shows mild increase and decrease at various regions. The water yield corresponding to IPSL CORDEX shows mild increase and IPSL SD has no change which are clearly due to the pattern of changes in precipitation. During winter season, the slight increase in the rainfall for EC-EARTH CORDEX is well reflected in the changes of water yield. In case of EC-EARTH SD and IPSL CORDEX, the changes in precipitation has more influence on the changes in water yield. It is also evident that increase in winter precipitation in MPI SD is the cause of increase in the water yield. The simulated water yield and projected precipitation for EC-EARTH SD is observed to have maximum increment. For all the sub-basins, the multi-climate model uncertainty dominates over the hydrological parameter uncertainty, and they are not even in comparable range.

Further, to understand the impact of GCM uncertainty and downscaling uncertainty over water balance projections, we have prepared a table showing the water balance projections for future and past, during each season of the year (Table 5). During the pre-monsoon season, precipitation shows a decrease across the model simulations, except

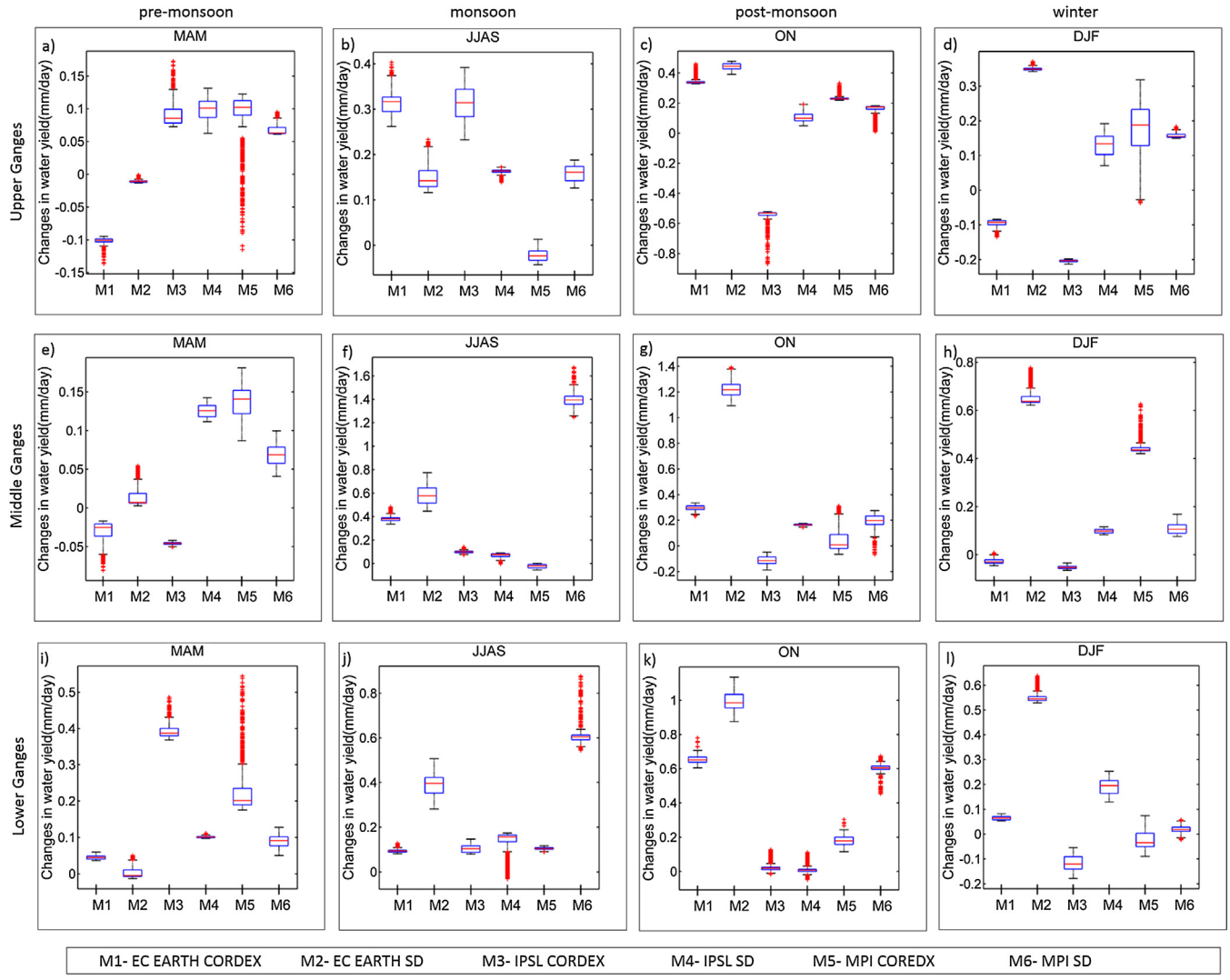

Fig. 13. Seasonal average of changes in simulated (calculated using Monte–Carlo simulations) water yields between the period of 2011–2037 and 1979–2005 for EC–EARTH CORDEX, EC–EARTH statistical downscaling (EC–EARTH SD), IPSL CORDEX, IPSL statistical downscaling (IPSL SD), MPI CORDEX (M5) and MPI statistical downscaling [(MPI SD), M6] for upper Ganga (a–d), middle Ganga (e–h), and lower Ganga (i–l).

IPSL SD and MPI CORDEX. There is an increase in evapotranspiration for IPSL CORDEX and IPSL SD. The dynamically downscaled data show increased water yield and decreased soil moisture changes. During the monsoon season, the precipitation decrease in all the simulations except MPI CORDEX. When all the simulations show an increase in evapotranspiration, IPSL CORDEX and MPI SD show a decline. The output corresponding to MPI CORDEX shows a reduced water yield. Other than IPSL SD, all other simulations show reduced change in soil moisture. The post monsoon precipitation is observed to decline except for that corresponding to IPSL CORDEX, IPSL SD and MPI SD. The evapotranspiration corresponding to IPSL SD, MPI CORDEX and MPI SD show a decline. Except for the simulation corresponding to IPSL CORDEX, water yield is observed to decline. The changes in soil moisture have become more prominent for MPI CORDEX simulations. EC SD, MPI CODEX and MPI SD show reduced winter precipitation. The change in evapotranspiration corresponding to EC EARTH CORDEX is negligible. Simulations of both the downscaled products of IPSL depict increased evapotranspiration. The CORDEX outputs of EC EARTH and IPSL are observed to show increased water yield when all the others are found to decrease. There is an overall decrease in the change in soil moisture across the winter season. Hence, it can be concluded that the deviation in the trend in precipitation for different GCMs and downscaling datasets is well reflected in the water balance projections.

In the present study, only the sensitive parameters were considered in the MCS. For a fairer comparison, all model parameters had to be considered to be uncertain. Therefore, a further analysis was performed by varying all the parameters in VIC viz. soil and vegetation parameters, following uniform distribution. The ranges for the parameters was procured from Bennett et al. (2018). We considered a range of ± 0.1 times the prescribed value for the parameters which were not considered in their study. The width of the band of simulated streamflow did not increase significantly and the model performance for extremes (low flow) is still bad in the new simulations (Fig. S1). The soil moisture and the ET plots are also quiet similar to the previous ones (Figs. S2 and S3). The uncertainty assessment did not bring much change in the spread of the output (Figs. S4–S6). The bias correction approach, followed in our study, is based on quantile mapping, developed by Li et al. (2010). It is a simple and straightforward technique that uses the difference between the CDFs derived from simulated and observed data. The difference is then used to adjust the model CDF to remove the bias. Although it has been widely employed in many studies, this method has certain limitations. It does not take into consideration the co-dependence of the GCM variables, since it corrects single variable at a time. Moreover, the bias correction is applied for a single time step without accounting for temporal oscillations (Mehrotra and Sharma, 2015). To examine whether a better bias correction

Table 5
Water balance projections during each season (MAM, JJAS, ON and DJF) averaged over 1979–2005 (past) and 2011–2037 (future).

Season	P (mm)	ET (mm)	R + B (mm)	ΔSM (mm)	Season	P (mm)	ET (mm)	R + B (mm)	ΔSM (mm)
EC-CORDEX					**EC-CORDEX**				
MAM-past	128.47	112.28	11.79	5.15	JJAS-past	1058.26	583.42	338.35	135.71
MAM-future	120.89	105.89	13.20	2.69	JJAS-future	1011.61	586.14	303.13	121.40
EC-SD					**EC-SD**				
MAM-past	70.32	86.49	8.22	−23.74	JJAS-past	930.85	541.60	217.71	171.22
MAM-future	62.53	66.91	6.24	−10.27	JJAS-future	901.76	596.83	177.55	125.10
IPSL-CORDEX					**IPSL-CORDEX**				
MAM-past	126.05	109.93	15.67	0.69	JJAS-past	983.83	562.32	289.31	130.44
MAM-future	124.55	122.23	17.84	−15.02	JJAS-future	940.35	555.15	266.05	117.16
IPSL-SD					**IPSL-SD**				
MAM-past	63.09	48.61	12.64	−2.78	JJAS-past	878.32	501.86	184.77	113.22
MAM-future	65.09	72.54	6.05	−13.23	JJAS-future	853.59	564.78	169.35	116.65
MPI-CORDEX					**MPI-CORDEX**				
MAM-past	80.88	76.45	13.16	−8.30	JJAS-past	917.00	476.14	296.26	144.12
MAM-future	81.39	71.77	14.11	−3.97	JJAS-future	938.42	493.39	299.92	143.63
MPI-SD					**MPI-SD**				
MAM-past	111.04	112.20	11.54	−12.32	JJAS-past	1010.17	574.15	283.67	150.45
MAM-future	60.54	71.56	5.58	−16.16	JJAS-future	929.92	567.14	217.38	143.42
EC-CORDEX					**EC-CORDEX**				
ON-past	150.22	171.22	70.05	−90.83	DJF-past	54.42	79.76	16.40	1.82
ON-future	124.78	160.65	54.79	−89.22	DJF-future	68.73	79.94	17.57	−0.61
EC-SD					**EC-SD**				
ON-past	105.21	142.39	69.31	−104.85	DJF-past	119.43	107.93	47.08	0.93
ON-future	44.78	117.16	24.06	−92.55	DJF-future	61.29	67.26	9.76	0.35
IPSL-CORDEX					**IPSL-CORDEX**				
ON-past	103.06	139.52	47.62	−81.36	DJF-past	39.89	72.43	9.30	0.75
ON-future	123.14	135.89	48.32	−58.45	DJF-future	76.01	94.08	18.53	−1.23
IPSL-SD					**IPSL-SD**				
ON-past	43.47	91.80	34.74	−82.64	DJF-past	63.71	60.16	15.14	1.17
ON-future	48.13	104.29	24.92	−77.16	DJF-future	68.39	77.68	10.83	1.11
MPI-CORDEX					**MPI-CORDEX**				
ON-past	67.96	123.65	50.93	−102.11	DJF-past	62.39	73.51	15.01	0.90
ON-future	65.51	125.54	47.87	−103.23	DJF-future	60.26	72.70	14.63	0.65
MPI-SD					**MPI-SD**				
ON-past	46.77	124.47	44.63	−118.33	DJF-past	87.44	83.12	16.99	1.13

accounting for variable dependence would reduce the uncertainty across GCMs, we used Multivariate Recursive Nested Bias Correction (MRNBC), developed by Mehrotra and Sharma (2015). The bias correction has been carried out for all the predictors for downscaling, viz. relative humidity, mean sea level pressure, temperature at surface and 500 hPa, uwind and vwind at surface and 500 hPa, for all the 3 GCMs. We compare the uncertainty in the simulated changes of the predictor variables for future, as obtained from both the bias correction methods. The results are presented in Fig. 14. We find that uncertainty is getting magnified even after introducing an improved bias correction method. This is consistently observed across all the variables except the Mean Sea Level Pressure (MSLP). This further strengthens our conclusion that the uncertainty across GCMs plays a major role in climate change impacts assessment over Indian monsoon region and reduction of such uncertainty is not even possible with the introduction of more sophisticated and accurate data driven models. This shows that one of the major challenge in hydrometeorology is the use of meteorological projections in hydrological applications. Though, there are multiple methods, such as multi-model averaging, Bayesian model averaging etc., to model uncertainty arising across climate models; the question remains on the confidence of using the simulations of changes of hydrological variables for water management and climate change adaptation.

4. Summary and conclusions

In the present study, we attempt to understand the uncertainty resulting from hydrological parameterization in the background of the uncertainty arising from the use of multiple climate models. We use the case study of Ganga basin, India, with the hydrological model, VIC. The hydrological parameter uncertainty is modelled with MCS. We find that, hydrological parameter uncertainty is almost negligible compared to the huge uncertainty resulting from the use of multiple GCMs and downscaling. Here, through MCS, we have considered all possible values of hydrological parameters. Hence, we may conclude that the possible error induced by a completely incorrect hydrological parametrization will be negligible compared to inter-climate model differences. Hence, from hydrological point of view, the multi-model climate change projections collectively do not provide any confidence to use them for adaptation. The uncertainty in GCMs may arise due to the multiple reasons such as the assumptions and parametrisation involved, model physics, no or limited knowledge about the future scenario and so on. When it comes to the downscaling techniques, the procedures followed in statistical and dynamic downscaling are entirely different. In statistical downscaling, the predictors and the predictand are related by a statistical relationship. In contrast to this, in dynamic downscaling, a regional climate model is run using the GCM output as boundary condition. Understanding the differences between the outputs of statistical and dynamic downscaling is complex and complicated task as dynamical downscaling is more intricate due to the involvement of regional climate model with huge number of parameterizations. This may be considered as the area of future research.

Usually, significant effort goes to the development of a hydrological model for a near correct estimation of the model parameters. This becomes even more challenging, when the model has limitations in some of the components of hydrological processes or some of the data is not available. As for example, for the present case, VIC does not have a ground water component that would lead to a good estimate of baseflow. This limitation can be overcome by coupling the VIC model with a groundwater model. Rosenberg et al. (2013) have attempted to couple the VIC model with a SIMple Groundwater Model (SIMGM) that represents the aquifer underlying the soil layers. However, it can be used

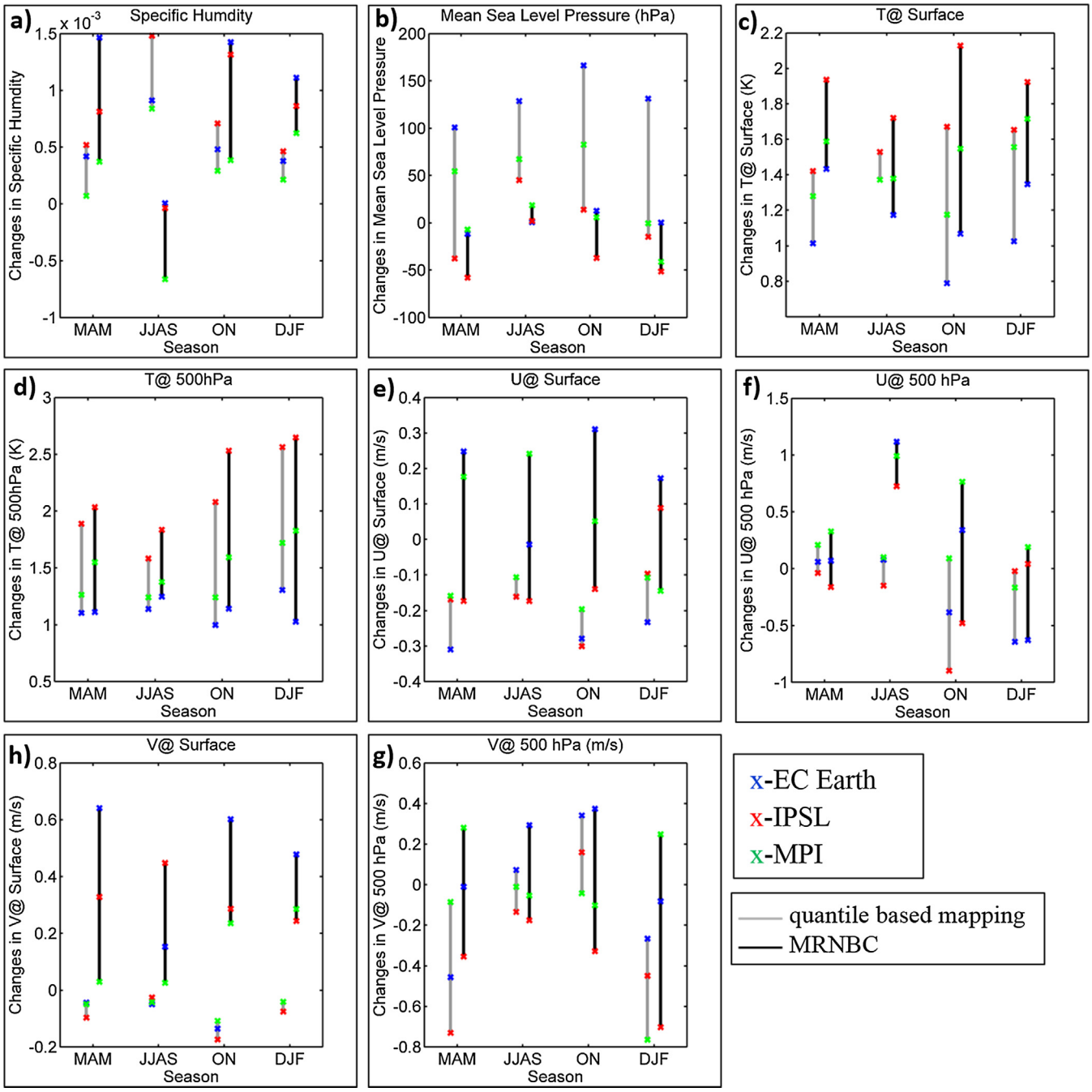

Fig. 14. Seasonal average of changes in predictor variables: (a) Specific humidity (b) Mean sea level pressure (hPa) (c) surface temperature (K) (d) temperature at 500 hPa (K) (e) u wind at surface (m/s) (f) u wind at 500 hPa (m/s) (g) v wind at surface (m/s) (h) v wind at 500 hPa (m/s) bias corrected using quantile based mapping and MRNBC respectively. The changes are calculated between a period 2011–2037 and 1979–2005 and averaged spatially over the Ganga Basin.

only for the study of changes in the total water storage as the model assumes arbitrary aquifer thickness. Therefore a more sophisticated groundwater model is required to be coupled to VIC model in order to include the groundwater interactions. Furthermore, the data related to ground water irrigation is neither available, nor the model has a good irrigation component representing the Indian agricultural practices. Calibrating an incomplete model based on streamflow may lead to a good match for a wrong reason. However, the question remains that even for a hypothetical ideal hydrological model, if significant efforts have been made to get all required data and perform parameterization with a huge effort, will that add value in climate change projections. We surprisingly arrive to a negative answer, and it attributes to the uncertain meteorological projections. Even after significant improvements in climate models and their physics, they are not good enough for a hydro-meteorological projections which can be used for climate adaptation with confidence. Negligible hydrological parameter uncertainty with respect to climate model uncertainty arrives to a conclusion that a poorly calibrated hydrological model, representing the hydrological processes wrong, has negligible error compared to inter-climate model uncertainty. However, it should be noted that in a hydrological sense these errors may be quite high and this gives the idea about the extent of poor agreements across climate models. This reduces the confidence of hydrologist to further use the projections for water management. The results do not say that hydrological parameterization is not required; rather emphasize on the urgent need of reducing uncertainty across climate models before providing any input to the water manager

community. It should be noted that recent literature (Mockler et al., 2016) also suggests that hydrological parameter uncertainty is on lower side compared to multi-model hydrological uncertainty (model structure uncertainty). This is a clear limitation of the present study and can be assessed by using multiple number of hydrological models as suggested by Moeck et al. (2016) and summarised in Smerdon (2017). Hence, the future scope of the work lies in the use of multiple hydrological models and comparison of the resulting uncertainty with the climate model uncertainty; however, the convergence of climate models is necessary for better hydrological impacts assessment and subsequent development of adaptation strategies.

Acknowledgement

Authors acknowledge the World Climate Research Programme's Working Group on Coupled Modelling, which is responsible for CMIP5 and climate modeling groups for producing and making available their model outputs. Authors acknowledge the Centre for Climate Change Research (CCCR-IITM) for RegCM4 and partner institutions (Institute for Atmospheric and Environmental Sciences (IAES), Germany for COSMO-CLM; Rossby Centre, Swedish Meteorological and Hydrological Institute (SMHI), Sweden for RCA4; Commonwealth Scientific and Industrial Research Organisation (CSIRO) for CCAM) for generating and disseminating the CORDEX South Asia multi-model dataset. Authors acknowledge Dr. J Sanjay, Dr. R Krishnan and Dr. Milind Mujumdar for providing their assistance in downloading CORDEX data. Authors also acknowledge Dr Kaustubh Salvi for providing statistical downscaled output. Authors acknowledge the associate editor and anonymous reviewers for reviewing the manuscript and providing constructive comments to improve the quality of the work. The authors sincerely thank the Ministry of Earth Sciences, Government of India, for funding the present work.

Appendix A. Supplementary data

Supplementary data associated with this article can be found, in the online version, at https://doi.org/10.1016/j.jhydrol.2018.08.080.

References

Allen, M.R., Stott, P.A., Mitchell, J.F.B., Schnur, R., Delworth, T.L., 2000. Quantifying the uncertainty in forecasts of anthropogenic climate change. Nature 407, 617–620. https://doi.org/10.1038/35036559.

Andreadis, K.M., Storck, P., Lettenmaier, D.P., 2009. Modeling snow accumulation and ablation processes in forested environments. Water Resour. Res. 45, 1–13. https://doi.org/10.1029/2008WR007042.

Arnell, N.W., 1999. Climate change scenarios for global impacts studies. Glob. Environ. Chang. 9. https://doi.org/10.1016/S0959-3780(99)00015-1.

Bae, D.-H., Jung, I.-W., Lettenmaier, D.P., 2011. Hydrologic uncertainties in climate change from IPCC AR4 GCM simulations of the Chungju Basin. Korea. J. Hydrol. 401, 90–105. https://doi.org/10.1016/j.jhydrol.2011.02.012.

Bastola, S., Murphy, C., Sweeney, J., 2011. The role of hydrological modelling uncertainties in climate change impact assessments of Irish river catchments. Adv. Water Resour. 34, 562–576. https://doi.org/10.1016/j.advwatres.2011.01.008.

Bennett, K.E., Urrego Blanco, J.R., Jonko, A., Bohn, T.J., Atchley, A.L., Urban, N.M., Middleton, R.S., 2018. Global sensitivity of simulated water balance indicators under future climate change in the colorado basin. Water Resour. Res. 54, 132–149. https://doi.org/10.1002/2017WR020471.

Bergström, S., Carlsson, B., Gardelin, M., Lindström, G., Petterson, A., Rummukainen, M., 2001. Climate change impacts on runoff in Sweden – assessments by global climate models, dynamical downscalling and hydrological modelling. Clim. Res. 16, 101–112. https://doi.org/10.3354/cr016101.

Beven, K., Binley, A., 1992. The future of distributed models: model calibration and uncertainty prediction. Hydrol. Process. 6, 279–298. https://doi.org/10.1002/hyp.3360060305.

Bosshard, T., Carambia, M., Goergen, K., Kotlarski, S., Krahe, P., Zappa, M., Schär, C., 2013. Quantifying uncertainty sources in an ensemble of hydrological climate-impact projections. Water Resour. Res. 49, 1523–1536. https://doi.org/10.1029/2011WR011533.

Chattopadhyay, N., Hulme, M., 1997. Evaporation and potential evapotranspiration in India under conditions of recent and future climate change. Agric. For. Meteorol. 87, 55–73. https://doi.org/10.1016/S0168-1923(97)00006-3.

Chawla, I., Mujumdar, P.P., 2015. Isolating the impacts of land use and climate change on streamflow. Hydrol. Earth Syst. Sci. 19, 3633–3651. https://doi.org/10.5194/hess-19-3633-2015.

Chen, H., Xu, C.-Y., Guo, S., 2012. Comparison and evaluation of multiple GCMs, statistical downscaling and hydrological models in the study of climate change impacts on runoff. J. Hydrol. 434, 36–45. https://doi.org/10.1016/j.jhydrol.2012.02.040.

Chen, J., Brissette, F.P., Leconte, R., 2011a. Uncertainty of downscaling method in quantifying the impact of climate change on hydrology. J. Hydrol. 401, 190–202. https://doi.org/10.1016/j.jhydrol.2011.02.020.

Chen, J., Brissette, F.P., Poulin, A., Leconte, R., 2011b. Overall uncertainty study of the hydrological impacts of climate change for a Canadian watershed. Water Resour. Res. 47, n/a-n/a. https://doi.org/10.1029/2011WR010602.

Chen, S.-T., Yu, P.-S., Tang, Y.-H., 2010. Statistical downscaling of daily precipitation using support vector machines and multivariate analysis. J. Hydrol. 385, 13–22. https://doi.org/10.1016/j.jhydrol.2010.01.021.

Christensen, N.S., Christensen, N.S., Wood, A.W., Wood, A.W., Voisin, N., Voisin, N., Lettenmaier, D.P., Lettenmaier, D.P., Palmer, R.N., Palmer, R.N., 2004. The effects of climate change on the hydrology and water resources of the colorado river basin. Clim. Change 62, 337–363. https://doi.org/10.1023/B:CLIM.0000013684.13621.1f.

Conway, D., Jones, P.D., 1998. The use of weather types and air flow indices for GCM downscaling. J. Hydrol. 212–213, 348–361. https://doi.org/10.1016/S0022-1694(98)00216-9.

Crosbie, R.S., Dawes, W.R., Charles, S.P., Mpelasoka, F.S., Aryal, S., Barron, O., Summerell, G.K., 2011. Differences in future recharge estimates due to GCMs, downscaling methods and hydrological models. Geophys. Res. Lett. 38, 1–5. https://doi.org/10.1029/2011GL047657.

Demaria, E.M., Nijssen, B., Wagener, T., 2007. Monte Carlo sensitivity analysis of land surface parameters using the Variable Infiltration Capacity model. J. Geophys. Res. 112, 1–15. https://doi.org/10.1029/2006JD007534.

Dobler, A., Ahrens, B., 2011. Four climate change scenarios for the Indian summer monsoon by the regional climate model COSMO-CLM. J. Geophys. Res. Atmos. 116, n/a-n/a. https://doi.org/10.1029/2011JD016329.

Dobler, A., Ahrens, B., 2010. Analysis of the Indian summer monsoon system in the regional climate model COSMO-CLM. J. Geophys. Res. 115, D16101. https://doi.org/10.1029/2009JD013497.

Dobler, C., Hagemann, S., Wilby, R.L., StÃtter, J., 2012. Quantifying different sources of uncertainty in hydrological projections in an Alpine watershed. Hydrol. Earth Syst. Sci. 16, 4343–4360. https://doi.org/10.5194/hess-16-4343-2012.

Döll, P., Kaspar, F., Lehner, B., 2003. A global hydrological model for deriving water availability indicators: Model tuning and validation. J. Hydrol. 270, 105–134. https://doi.org/10.1016/S0022-1694(02)00283-4.

Döll, P., Berkhoff, K., Bormann, H., Fohrer, N., Gerten, D., Hagemann, S., Krol, M., 2008. Advances and visions in large-scale hydrological modelling: findings from the 11th workshop on large-scale hydrological modelling. Adv. Geosci. 18, 51–61. https://doi.org/10.5194/adgeo-18-51-2008.

Dosio, A., Panitz, H.-J., Schubert-Frisius, M., Lüthi, D., 2015. Dynamical downscaling of CMIP5 global circulation models over CORDEX-Africa with COSMO-CLM: evaluation over the present climate and analysis of the added value. Clim. Dyn. 44, 2637–2661. https://doi.org/10.1007/s00382-014-2262-x.

Fan, Y., Miguez-Macho, G., Weaver, C.P., Walko, R., Robock, A., 2007. Incorporating water table dynamics in climate modeling: 1. Water table observations and equilibrium water table simulations. J. Geophys. Res. 112, D10125. https://doi.org/10.1029/2006JD008111.

Flaounas, E., Drobinski, P., Vrac, M., Bastin, S., Lebeaupin-Brossier, C., Stéfanon, M., Borga, M., Calvet, J.-C., 2013. Precipitation and temperature space–time variability and extremes in the Mediterranean region: evaluation of dynamical and statistical downscaling methods. Clim. Dyn. 40, 2687–2705. https://doi.org/10.1007/s00382-012-1558-y.

Fowler, H.J., Blenkinsop, S., Tebaldi, C., 2007. Linking climate change modelling to impacts studies: recent advances in downscaling techniques for hydrological modelling. Int. J. Climatol. 27, 1547–1578. https://doi.org/10.1002/joc.1556.

Ghosh, S., Katkar, S., 2012. Modeling uncertainty resulting from multiple downscaling methods in assessing hydrological impacts of climate change. Water Resour. Manag. 26, 3559–3579. https://doi.org/10.1007/s11269-012-0090-5.

Ghosh, S., Mujumdar, P.P., 2009. Climate change impact assessment: Uncertainty modeling with imprecise probability. J. Geophys. Res. Atmos. 114. https://doi.org/10.1029/2008JD011648.

Ghosh, S., Mujumdar, P.P., 2007. Nonparametric methods for modeling GCM and scenario uncertainty in drought assessment. Water Resour. Res. 43, 1–19. https://doi.org/10.1029/2006WR005351.

Ghosh, S., Vittal, H., Sharma, T., Karmakar, S., Kasiviswanathan, K.S., Dhanesh, Y., Sudheer, K.P., Gunthe, S.S., 2016. Indian summer monsoon rainfall: implications of contrasting trends in the spatial variability of means and extremes. PLoS One 11, e0158670. https://doi.org/10.1371/journal.pone.0158670.

Gleick, P.H., 1986. Methods for evaluating the regional hydrologic impacts of global climate. Changes 88, 97–116.

Gosain, A.K., Rao, S., Basuray, D., 2006. Climate change impact assessment on hydrology of Indian river basins. Current 90, 346–353.

Groppelli, B., Bocchiola, D., Rosso, R., 2011. Spatial downscaling of precipitation from GCMs for climate change projections using random cascades: a case study in Italy. Water Resour. Res. 47, n/a-n/a. https://doi.org/10.1029/2010WR009437.

Gutmann, E., Pruitt, T., Clark, M.P., Brekke, L., Arnold, J.R., Raff, D.A., Rasmussen, R.M., 2014. An intercomparison of statistical downscaling methods used for water resource assessments in the United States. Water Resour. Res. 50, 7167–7186. https://doi.org/10.1002/2014WR015559.

Haddeland, I., Lettenmaier, D.P., Skaugen, T., 2006a. Effects of irrigation on the water and energy balances of the Colorado and Mekong river basins. J. Hydrol. 324,

210–223. https://doi.org/10.1016/j.jhydrol.2005.09.028.
Haddeland, I., Skaugen, T., Lettenmaier, D.P., 2006b. Anthropogenic impacts on continental surface water fluxes. Geophys. Res. Lett. 33, 2–5. https://doi.org/10.1029/2006GL026047.
Hamlet, A.F., Lettenmaier, D.P., 1999. Global observed changes in daily climate extremes of temperature and precipitation. J. Geophys. Res. Atmos. 35, 1597–1623. https://doi.org/10.1029/2005JD006290.
Hansen, M.C., Defries, R.S., Townshend, J.R.G., Sohlberg, R., 2000. Global land cover classification at 1 km spatial resolution using a classification tree approach. Int. J. Remote Sens. 21, 1331–1364. https://doi.org/10.1080/014311600210209.
Hingray, B., Saïd, M., Hingray, B., Saïd, M., 2014. Partitioning internal variability and model uncertainty components in a multimember multimodel ensemble of climate projections. J. Clim. 27, 6779–6798. https://doi.org/10.1175/JCLI-D-13-00629.1.
Hu, Y., Maskey, S., Uhlenbrook, S., 2013. Downscaling daily precipitation over the Yellow River source region in China: a comparison of three statistical downscaling methods. Theor. Appl. Climatol. 112, 447–460. https://doi.org/10.1007/s00704-012-0745-4.
Hughes, J.P., Lettenmaier, D.P., Guttorp, P., 1993. A stochastic approach for assessing the effect of changes in synoptic circulation patterns on gauge precipitation. Water Resour. Res. 29, 3303–3315. https://doi.org/10.1029/93WR01066.
Im, E.-S., Jung, I.-W., Chang, H., Bae, D.-H., Kwon, W.-T., 2010. Hydroclimatological response to dynamically downscaled climate change simulations for Korean basins. Clim. Change 100, 485–508. https://doi.org/10.1007/s10584-009-9691-2.
Jaramillo, F., Destouni, G., 2015. Local flow regulation and irrigation raise global human water consumption and footprint. Science 350, 1248–1251. https://doi.org/10.1126/science.aad1010.
Jeong, D.I., St-Hilaire, A., Ouarda, T.B.M.J., Gachon, P., 2012. Multisite statistical downscaling model for daily precipitation combined by multivariate multiple linear regression and stochastic weather generator. Clim. Change 114, 567–591. https://doi.org/10.1007/s10584-012-0451-3.
Jiang, T., Chen, Y.D., Xu, C., Chen, X., Chen, X., Singh, V.P., 2007. Comparison of hydrological impacts of climate change simulated by six hydrological models in the Dongjiang Basin, South China. J. Hydrol. 336, 316–333. https://doi.org/10.1016/j.jhydrol.2007.01.010.
Jones, R.G., Murphy, J.M., Noguer, M., 1995. Simulation of climate change over europe using a nested regional-climate model. I: Assessment of control climate, including sensitivity to location of lateral boundaries. Q. J. R. Meteorol. Soc. 121, 1413–1449. https://doi.org/10.1002/qj.49712152610.
Kannan, S., Ghosh, S., 2013. A nonparametric kernel regression model for downscaling multisite daily precipitation in the Mahanadi basin. Water Resour. Res. 49, 1360–1385. https://doi.org/10.1002/wrcr.20118.
Kannan, S., Ghosh, S., Mishra, V., Salvi, K., 2014. Uncertainty resulting from multiple data usage in statistical downscaling. Geophys. Res. Lett. 41, 4013–4019. https://doi.org/10.1002/2014GL060089.
Khan, M.S., Coulibaly, P., Dibike, Y., 2006. Uncertainty analysis of statistical downscaling methods. J. Hydrol. 319, 357–382. https://doi.org/10.1016/j.jhydrol.2005.06.035.
Kim, H.W., Hwang, K., Mu, Q., Lee, S.O., Choi, M., 2012. Validation of MODIS 16 global terrestrial evapotranspiration products in various climates and land cover types in Asia. KSCE J. Civ. Eng. 16, 229–238. https://doi.org/10.1007/s12205-012-0006-1.
Koshal, A.K., 2014. Changing current scenario of rice-wheat system in indo-gangetic plain region of India. Int. J. Sci. Res. Publ. 4, 1–13.
Krishna Kumar, K., Patwardhan, S.K., Kulkarni, A., Kamala, K., Koteswara Rao, K., Jones, R., 2011. Simulated projections for summer monsoon climate over India by a high-resolution regional climate model (PRECIS). Curr. Sci. 101, 312–326.
Kumar, K.R., Pant, G.B., Parthasarathy, B., Sontakke, N., a, 1992. Spatial and subseasonal patterns of the long-term trends of Indian summer monsoon rainfall. Int. J. Climatol. 12, 257–268. https://doi.org/10.1002/joc.3370120303.
Kumar, P., Wiltshire, A., Mathison, C., Asharaf, S., Ahrens, B., Lucas-Picher, P., Christensen, J.H., Gobiet, A., Saeed, F., Hagemann, S., Jacob, D., 2013. Downscaled climate change projections with uncertainty assessment over India using a high resolution multi-model approach. Sci. Total Environ. 468, S18–S30. https://doi.org/10.1016/j.scitotenv.2013.01.051.
Leavesley, G.H., 1994. Modeling the effects of climate change on water resources – a review. Clim. Change 28, 159–177. https://doi.org/10.1007/BF01094105.
Lee, J.H., Kim, C.J., 2013. A multimodel assessment of the climate change effect on the drought severity-duration-frequency relationship. Hydrol. Process. 27, 2800–2813. https://doi.org/10.1002/hyp.9390.
Leng, G., Huang, M., Tang, Q., Gao, H., Leung, L.R., 2014. Modeling the effects of groundwater-fed irrigation on terrestrial hydrology over the conterminous United States. J. Hydrometeorol. 15, 957–972. https://doi.org/10.1175/JHM-D-13-049.1.
Lettenmaier, D.P., Gan, T.Y., 1990. Hydrologic sensitivities of the Sacramento-San Joaquin River Basin, California, to global warming. Water Resour. Res. 26, 69–86. https://doi.org/10.1029/WR026i001p00069.
Li, H., Sheffield, J., Wood, E.F., 2010. Bias correction of monthly precipitation and temperature fields from Intergovernmental Panel on Climate Change AR4 models using equidistant quantile matching. J. Geophys. Res. Atmos. 115. https://doi.org/10.1029/2009JD012882.
Liang, X., 2003. A new parameterization for surface and groundwater interactions and its impact on water budgets with the variable infiltration capacity (VIC) land surface model. J. Geophys. Res. 108. https://doi.org/10.1029/2002JD003090.
Liang, X., Lettenmaier, D.P., Wood, E.F., Burges, S.J., 1994. A simple hydrologically based model of land surface water and energy fluxes for general circulation models. J. Geophys. Res. 99, 14415. https://doi.org/10.1029/94JD00483.
Liang, X., Wood, E.F., Lettenmaier, D.P., 1996. Surface soil moisture parameterization of the VIC-2L model: Evaluation and modification. Glob. Planet. Change 13, 195–206. https://doi.org/10.1016/0921-8181(95)00046-1.
Liu, S., Gao, W., Liang, X.-Z., 2013. A regional climate model downscaling projection of China future climate change. Clim. Dyn. 41, 1871–1884. https://doi.org/10.1007/s00382-012-1632-5.
Lohmann, D., Raschke, E., Nijssen, B., Lettenmaier, D.P., 1998. Regional scale hydrology: I. Formulation of the VIC-2L model coupled to a routing model. Hydrol. Sci. J. 43, 131–141. https://doi.org/10.1080/02626669809492107.
Maurer, E.P., Duffy, P.B., 2005. Uncertainty in projections of streamflow changes due to climate change in California. Geophys. Res. Lett. 32, 1–5. https://doi.org/10.1029/2004GL021462.
Mehrotra, R., Sharma, A., 2015. Correcting for systematic biases in multiple raw GCM variables across a range of timescales. J. Hydrol. 520, 214–223. https://doi.org/10.1016/j.jhydrol.2014.11.037.
Milly, P.C.D., Dunne, K., a, Vecchia, a V, 2005. Global pattern of trends in streamflow and water availability in a changing climate. Nature 438, 347–350. https://doi.org/10.1038/nature04312.
Mishra, V., 2015. Climatic uncertainty in Himalayan water towers. J. Geophys. Res. Atmos. 120, 2689–2705. https://doi.org/10.1002/2014JD022650.
Mishra, V., Cherkauer, K.A., Shukla, S., 2010. Assessment of drought due to historic climate variability and projected future climate change in the midwestern United States. J. Hydrometeorol. 11, 46–68. https://doi.org/10.1175/2009JHM1156.1.
Mockler, E.M., Chun, K.P., Sapriza-Azuri, G., Bruen, M., Wheater, H.S., 2016. Assessing the relative importance of parameter and forcing uncertainty and their interactions in conceptual hydrological model simulations. Adv. Water Resour. https://doi.org/10.1016/j.advwatres.2016.10.008.
Moeck, C., Brunner, P., Hunkeler, D., 2016. The influence of model structure on groundwater recharge rates in climate-change impact studies. Hydrogeol. J. 24, 1171–1184. https://doi.org/10.1007/s10040-016-1367-1.
Moradkhani, H., Sorooshian, S., 2009. General review of rainfall-runoff modeling: model calibration, data assimilation, and uncertainty analysis. Rev. Lit. Arts Am. 63, 1–24. https://doi.org/10.1007/978-3-540-77843-1_1.
Mujumdar, P.P., Ghosh, S., 2008. Modeling GCM and scenario uncertainty using a possibilistic approach: application to the Mahanadi River. India. Water Resour. Res. 44, 1–15. https://doi.org/10.1029/2007WR006137.
Muleta, M.K., Nicklow, J.W., 2005. Sensitivity and uncertainty analysis coupled with automatic calibration for a distributed watershed model. J. Hydrol. 306, 127–145. https://doi.org/10.1016/j.jhydrol.2004.09.005.
New, M., Hulme, M., 2000. Representing uncertainty in climate change scenarios: a Monte-Carlo approach. Integr. Assess. 1, 203–213. https://doi.org/10.1023/A:1019144202120.
B. Nijssen, D.P. Lettenmaier, X. Liang, S.W. Wetzel, E.F. Wood, 1997. Streamflow simulation for continental-scale river basins and radiative forcings) applications of the model to the Columbia and annual flow volumes to within a few percent . Difficulties in reproducing the Sa6ramento Model [Burnash is dominated using an 33, 711–724.
Nijssen, B., O'Donnell, G.M., Lettenmaier, D.P., Lohmann, D., Wood, E.F., 2001a. Predicting the discharge of global rivers. J. Clim. 14, 3307–3323. https://doi.org/10.1175/1520-0442(2001) 014<3307:PTDOGR>2.0.CO;2.
Nijssen, B., Schnur, R., Lettenmaier, D.P., 2001b. Global retrospective estimation of soil moisture using the variable infiltration capacity land surface modl, 1980–93. J. Clim. 14, 1790–1808. https://doi.org/10.1175/1520-0442(2001) 014<1790:GREOSM>2.0.CO;2.
Moef, N.R.C.D., 2009. Status paper on river ganga – state of environment and water quality. Altern. Hydro Energy Cent. Indian Inst. Technol. Roorkee 1–38.
Oki, T., Kanae, S., 2006. Global Hydrological Cycles and. Science (80-.) 313, 1068–1072.
Osca, J., Romero, R., Alonso, S., 2013. Precipitation projections for Spain by means of a weather typing statistical method. Glob. Planet. Change 109, 46–63. https://doi.org/10.1016/j.gloplacha.2013.08.001.
Prudhomme, C., Jakob, D., Svensson, C., 2003. Uncertainty and climate change impact on the flood regime of small UK catchments. J. Hydrol. 277, 1–23. https://doi.org/10.1016/S0022-1694(03)00065-9.
Prudhomme, C., Reynard, N., Crooks, S., 2002. Downscaling of global climate models for flood frequency analysis: where are we now? Hydrol. Process. 16, 1137–1150. https://doi.org/10.1002/hyp.1054.
Raje, D., Krishnan, R., 2012. Bayesian parameter uncertainty modeling in a macroscale hydrologic model and its impact on Indian river basin hydrology under climate change. Water Resour. Res. 48, 1–17. https://doi.org/10.1029/2011WR011123.
Raje, D., Mujumdar, P.P., 2009. A conditional random field-based downscaling method for assessment of climate change impact on multisite daily precipitation in the Mahanadi basin. Water Resour. Res. 45, n/a-n/a. https://doi.org/10.1029/2008WR007487.
Raje, D., Priya, P., Krishnan, R., 2014. Macroscale hydrological modelling approach for study of large scale hydrologic impacts under climate change in Indian river basins. Hydrol. Process. 28, 1874–1889. https://doi.org/10.1002/hyp.9731.
Rajeevan, M., Bhate, J., 2009. A high resolution gridded rainfall dataset (1971–2005) for mesoscale meteorological studies. Curr. Sci. 96, 558–562.
Rajeevan, M., Bhate, J., Kale, J.D., Lal, B., 2006. High resolution daily gridded rainfall data for the Indian region: Analysis of break and active monsoon spells. Curr. Sci. 91, 296–306.
Ramoelo, A., Majozi, N., Mathieu, R., Jovanovic, N., Nickless, A., Dzikiti, S., 2014. Validation of Global Evapotranspiration Product (MOD16) using Flux Tower Data in the African Savanna. South Africa. Remote Sens. 6, 7406–7423. https://doi.org/10.3390/rs6087406.
Refsgaard, J., Sonnenborg, T., Butts, M., Christensen, J., Christensen, S., Drews, M., Jensen, K., Jørgensen, F., Jørgensen, L., Larsen, M., Rasmussen, S., Seaby, L., Seifert, D., Vilhelmsen, T., 2016. Climate change impacts on groundwater hydrology – where are the main uncertainties and can they be reduced? Hydrol. Sci. J. 6, 2312–2324. https://doi.org/10.1080/02626667.2015.1131899.
Refsgaard, J.C., Arnbjerg-Nielsen, K., Drews, M., Halsnæs, K., Jeppesen, E., Madsen, H.,

Markandya, A., Olesen, J.E., Porter, J.R., Christensen, J.H., 2013. The role of uncertainty in climate change adaptation strategies—A Danish water management example. Mitig. Adapt. Strateg. Glob. Chang. 18, 337–359. https://doi.org/10.1007/s11027-012-9366-6.

Rosenberg, E.A., Clark, E.A., Steinemann, A.C., Lettenmaier, D.P., 2013. On the contribution of groundwater storage to interannual streamflow anomalies in the Colorado River basin. Hydrol. Earth Syst. Sci. 17, 1475–1491. https://doi.org/10.5194/hess-17-1475-2013.

Ruelland, D., Hublart, P., Tramblay, Y., 2015. Assessing uncertainties in climate change impacts on runoff in Western Mediterranean basins. Proc. Int. Assoc. Hydrol. Sci. 371, 75–81. https://doi.org/10.5194/piahs-371-75-2015.

Sachindra, D.A., Huang, F., Barton, A., Perera, B.J.C., 2013. Least square support vector and multi-linear regression for statistically downscaling general circulation model outputs to catchment streamflows. Int. J. Climatol. 33, 1087–1106. https://doi.org/10.1002/joc.3493.

Salvi, K., Kannan, S., Ghosh, S., 2013. High-resolution multisite daily rainfall projections in India with statistical downscaling for climate change impacts assessment. J. Geophys. Res. Atmos. 118, 3557–3578. https://doi.org/10.1002/jgrd.50280.

Samadi, S., Wilson, C.A.M.E., Moradkhani, H., 2013. Uncertainty analysis of statistical downscaling models using Hadley Centre Coupled Model. Theor. Appl. Climatol. 114, 673–690. https://doi.org/10.1007/s00704-013-0844-x.

Santos, J.A., Belo-Pereira, M., Fraga, H., Pinto, J.G., 2016. Understanding climate change projections for precipitation over western Europe with a weather typing approach. J. Geophys. Res. Atmos. 121, 1170–1189. https://doi.org/10.1002/2015JD024399.

Scinocca, J.F., Kharin, V.V., Jiao, Y., Qian, M.W., Lazare, M., Solheim, L., Flato, G.M., Biner, S., Desgagne, M., Dugas, B., Scinocca, J.F., Kharin, V.V., Jiao, Y., Qian, M.W., Lazare, M., Solheim, L., Flato, G.M., Biner, S., Desgagne, M., Dugas, B., 2016. Coordinated Global and Regional Climate Modeling*. J. Clim. 29, 17–35. https://doi.org/10.1175/JCLI-D-15-0161.1.

Seneviratne, S.I., Corti, T., Davin, E.L., Hirschi, M., Jaeger, E.B., Lehner, I., Orlowsky, B., Teuling, A.J., 2010. Investigating soil moisture-climate interactions in a changing climate: a review. Earth-Science Rev. 99, 125–161. https://doi.org/10.1016/j.earscirev.2010.02.004.

Simonovic, S.P., Asce, M., Li, L., 2003. Methodology for Assessment of Climate Change Impacts on Large-Scale Flood Protection. System 129, 361–371.

Simonovic, S.P., Li, L., 2004. Sensitivity of the Red River Basin Flood Protection System to Climate Variability and. Change, pp. 89–110.

Singh, P., Kumar, N., 1997. Impact assessment of climate change on the hydrological response of a snow and glacier melt runoff dominated Himalayan river. J. Hydrol. 193, 316–350. https://doi.org/10.1016/S0022-1694(96)03142-3.

Singh, S., Ghosh, S., Sahana, A.S., Vittal, H., Karmakar, S., 2016. Do dynamic regional models add value to the global model projections of Indian monsoon? Clim. Dyn. 1–23. https://doi.org/10.1007/s00382-016-3147-y.

Smerdon, B.D., 2017. A synopsis of climate change effects on groundwater recharge. J. Hydrol. 555, 125–128. https://doi.org/10.1016/j.jhydrol.2017.09.047.

Srivastava, A., Rajeevan, M., Kshirsagar, S., 2009. Development of a high resolution daily gridded temperature data set (1969–2005) for the Indian region. Atmos. Sci. Lett. 10, 249–254. https://doi.org/10.1002/asl.

Stoll, S., Hendricks Franssen, H.J., Butts, M., Kinzelbach, W., 2011. Analysis of the impact of climate change on groundwater related hydrological fluxes: A multi-model approach including different downscaling methods. Hydrol. Earth Syst. Sci. 15, 21–38. https://doi.org/10.5194/hess-15-21-2011.

Syed, T.H., Webster, P.J., Famiglietti, J.S., 2014. Assessing variability of evapotranspiration over the Ganga river basin using water balance computations. Water Resour. Res. 50, 2551–2565. https://doi.org/10.1002/2013WR013518.

Taylor, K.E., Stouffer, R.J., Meehl, G.A., 2012. An overview of CMIP5 and the experiment design. Bull. Am. Meteorol. Soc. 93, 485–498. https://doi.org/10.1175/BAMS-D-11-00094.1.

Tebaldi, C., Smith, R.L., Nychka, D., Mearns, L.O., 2005. Quantifying uncertainty in projections of regional climate change: a bayesian approach to the analysis of multimodel ensembles. J. Clim. 18, 1524–1540. https://doi.org/10.1175/JCLI3363.1.

Teng, J., Vaze, J., Chiew, F.H.S., Wang, B., Perraud, J.-M., 2012. Estimating the relative uncertainties sourced from GCMs and hydrological models in modeling climate change impact on runoff. J. Hydrometeorol. 13, 122–139. https://doi.org/10.1175/JHM-D-11-058.1.

Teutschbein, C., Wetterhall, F., Seibert, J., 2011. Evaluation of different downscaling techniques for hydrological climate-change impact studies at the catchment scale. Clim. Dyn. 37, 2087–2105. https://doi.org/10.1007/s00382-010-0979-8.

Trenberth, K.E., Dai, A., Rasmussen, R.M., Parsons, D.B., 2003. The changing character of precipitation. 1205–1217 + 1161. Bull. Am. Meteorol. Soc. 84. https://doi.org/10.1175/BAMS-84-9-1205.

Troy, T.J., Wood, E.F., Sheffield, J., 2008. An efficient calibration method for continental-scale land surface modeling. Water Resour. Res. 44, 1–13. https://doi.org/10.1029/2007WR006513.

Vaittinada Ayar, P., Vrac, M., Bastin, S., Carreau, J., Déqué, M., Gallardo, C., 2016. Intercomparison of statistical and dynamical downscaling models under the EURO- and MED-CORDEX initiative framework: present climate evaluations. Clim. Dyn. 46, 1301–1329. https://doi.org/10.1007/s00382-015-2647-5.

Velázquez, J.A., Schmid, J., Ricard, S., Muerth, M.J., Gauvin St-Denis, B., Minville, M., Chaumont, D., Caya, D., Ludwig, R., Turcotte, R., 2013. An ensemble approach to assess hydrological models' contribution to uncertainties in the analysis of climate change impact on water resources. Hydrol. Earth Syst. Sci. 17, 565–578. https://doi.org/10.5194/hess-17-565-2013.

C.J. Vorosmarty, B. Moore, 1991. Modeling basin-scale hydrology in support of physical climate and global biogeochemical studies: an example using the Zambi River 271–311.

Wilby, R.L., 2005. Uncertainty in water resource model parameters used for climate change impact assessment. Hydrol. Process. 19, 3201–3219. https://doi.org/10.1002/hyp.5819.

Wilby, R.L., Harris, I., 2006. A framework for assessing uncertainties in climate change impacts: low-flow scenarios for the River Thames. UK. Water Resour. Res. 42, 1–10. https://doi.org/10.1029/2005WR004065.

Wild, M., Liepert, B., 2010. The Earth radiation balance as driver of the global hydrological cycle. Environ. Res. Lett. 5, 25203. https://doi.org/10.1088/1748-9326/5/2/025203.

Willmott, C.J., Robeson, S.M., Matsuura, K., 2012. A refined index of model performance. Int. J. Climatol. 32, 2088–2094. https://doi.org/10.1002/joc.2419.

Woldemeskel, F.M., Sharma, A., Sivakumar, B., Mehrotra, R., 2016. Quantification of precipitation and temperature uncertainties simulated by CMIP3 and CMIP5 models. J. Geophys. Res. Atmos. 121, 3–17. https://doi.org/10.1002/2015JD023719.

Woldemeskel, F.M., Sharma, A., Sivakumar, B., Mehrotra, R., 2014. A framework to quantify GCM uncertainties for use in impact assessment studies. J. Hydrol. 519, 1453–1465. https://doi.org/10.1016/j.jhydrol.2014.09.025.

Xu, C., 1999. Climate Change and Hydrologic Models : A Review of Existing Gaps and Recent Research Developments. Water Resour. Manag. 13, 369–382. https://doi.org/10.1023/A:1008190900459.

Yapo, P.O., Gupta, H.V., Sorooshian, S., 1996. Automatic calibration of conceptual rainfall-runoff models: sensitivity to calibration data. J. Hydrol. 181, 23–48. https://doi.org/10.1016/0022-1694(95)02918-4.

Yip, S., Ferro, C.A.T., Stephenson, D.B., Hawkins, E., Yip, S., Ferro, C.A.T., Stephenson, D.B., Hawkins, E., 2011. A Simple, Coherent Framework for Partitioning Uncertainty in Climate Predictions. J. Clim. 24, 4634–4643. https://doi.org/10.1175/2011JCLI4085.1.